Ptf1a/Rbpj complex inhibits ganglion cell fate and drives the specification of all horizontal cell subtypes in the chick retina.

E.C. Lelièvre[1,2,3,4,5], M. Lek[6], H. Boije[6], L. Houille-Vernes[2,4,5], V. Brajeul[2,4,5], A. Slembrouck[2,4,5], J.E. Roger[4], J. Sahel[2,4,5], J.M. Matter[7], F. Sennlaub[1,2,3], F. Hallböök[6], O. Goureau[2,4,5*] and X. Guillonneau[1,2,3]*.

1-Centre de Recherche des Cordeliers, INSERM UMR S872, 75006 Paris, France

2-Université Pierre et Marie Curie, 75006 Paris, France

3-Université Paris Descartes, 75006, Paris, France

4-Institut de la Vision, INSERM UMR S968, 75012 Paris, France

5- CNRS UMR 7210, 75012, Paris, France

6- Department of Neuroscience, Biomedical Centre, Uppsala University, Husargatan 3, Uppsala, Sweden.

7- Department of Biochemistry, Sciences II, University of Geneva, 1211 Genève 4, Switzerland.

**Corresponding authors*

Xavier Guillonneau

Centre de Recherche des Cordeliers, UMR S872, Equipe 21

15, Rue de L'Ecole de Médecine, 75006 Paris, France.

Tel: (33) 1.44.27.80.87 Fax: (33) 1.44.27.40.92

Email: xavier.guillonneau@inserm.fr

Olivier Goureau

Institut de la Vision, UMR S869, Equipe 3

12, Rue Moreau, 75012 Paris, France.

Tel : (33) 1.53.46.25.32 Fax : (33) 1.53.46.26.01

Email : olivier.goureau@inserm.fr

Running Title: Ptf1a in chick retinal development

ABSTRACT

During development, progenitor cells of the retina give rise to six principal classes of neurons and the Müller glial cells found within the adult retina. The pancreas transcription factor 1 subunit a (Ptf1a) encodes a basic-helix-loop-helix transcription factor necessary for the specification of horizontal cells and the majority of amacrine cell subtypes in the mouse retina. The Ptf1a-regulated genes and the regulation of Ptf1a activity by transcription cofactors during retinogenesis have been poorly investigated. Using a retrovirus-mediated gene transfer approach, we reported that Ptf1a was sufficient to promote the fates of amacrine and horizontal cells from retinal progenitors and inhibit retinal ganglion cell and photoreceptor differentiation in the chick retina. Both GABAergic H1 and non-GABAergic H3 horizontal cells were induced following the forced expression of Ptf1a. We describe Ptf1a as a strong, negative regulator of Atoh7 expression. Furthermore, the Rbpj-interacting domains of Ptf1a protein were required for its effects on cell fate specification. Together, these data provide a novel insight into the molecular basis of Ptf1a activity on early cell specification in the chick retina.

Key words: Cell specification, Horizontal cell, Atoh7/Ath5, retina, chick.

INTRODUCTION

The vertebrate neural retina is a laminar structure composed of six types of neurons and one major type of glial cells, the Müller cells. The seven cell types are derived from a common pool of multipotent retinal progenitor cells (RPC) that differentiate in a conserved chronological order. Retinal ganglion cells, cones, horizontal (HC) and amacrine (AC) cells are produced first, whereas rods, Müller glial cells and bipolar cells are generated last (Prada et al., 1991; Young, 1985). The RPC differentiation pathway choice is determined by cell-intrinsic, i.e., transcription factors, and cell-extrinsic factors (Livesey and Cepko, 2001; Marquardt and Gruss, 2002; Ohsawa and Kageyama, 2008).

Ptf1a encodes a basic-helix-loop-helix (bHLH) transcription factor that drives undifferentiated cells in the foregut to differentiate into a pancreatic lineage during pancreas development (Kawaguchi et al., 2002; Krapp et al., 1998). Ptf1a is also expressed during the development of many structures of the central nervous system (Glasgow et al., 2005; Zecchin et al., 2004). In the cerebellum and the spinal cord, Ptf1a is expressed in the precursors of GABAergic neurons, and the loss of *Ptf1a* induced these GABAergic neurons to adopt a glutamatergic phenotype (Glasgow et al., 2005; Hoshino et al., 2005; Pascual et al., 2007). In the retina, Ptf1a acts as an HC and AC fate determination factor at the expense of ganglion cells in mice, zebrafish and *Xenopus* (Dong et al., 2008; Dullin et al., 2007; Fujitani et al., 2006; Nakhai et al., 2007) and of photoreceptors in zebrafish and *Xenopus* (Dong et al., 2008; Dullin et al., 2007). These studies have thoroughly characterized the phenotypic modifications induced by Ptf1a loss- and gain-of-function in the retina, but the molecular mechanisms underlying Ptf1a activity are not as well understood. Loss-of-function studies reported a change in the expression of a set of retinogenic factors in the *Ptf1a*-null retinas (Fujitani et al., 2006; Nakhai et al., 2007). Nevertheless, because some of these factors are persistently expressed in mature cells, it remains to be established if these changes were due to specific

transcriptional regulations or qualitative changes in the cell populations expressing these factors.

Unlike other class II bHLH transcription factors, Ptf1a functions in the pancreas as part of a trimeric complex. The pancreas transcription factor 1 complex (PTF1) includes Ptf1a, a ubiquitous class I bHLH transcription factor (E-protein) and the mammalian Suppressor of Hairless protein, Rbpj (PTF1-J complex) or its paralog, Rbpjl (PTF1-L complex) (Beres et al., 2006; Masui et al., 2007; Obata et al., 2001). The Ptf1a-Rbpj interaction is also required for Ptf1a to specify GABAergic cells in the dorsal spinal cord and the cerebellum (Hori et al., 2008). However, the requirement of the Ptf1a-Rbpj interaction in the specification of retinal cell types remains to be elucidated.

The chick retina has proven to be a powerful model to study retinal differentiation and its genetic regulation. Moreover, in contrast to mice possessing only one axon-bearing HC subtype (Peichl and Gonzalez-Soriano, 1994), the chick retina has both axon-less and axon-bearing HC subtypes, as found in the majority of vertebrate retinas (Gallego, 1986; Genis-Galvez, 1979). The chick retina contains H1 axon-bearing HCs, H2 axon-less “stellate” HCs and H3 axon-less “candelabrum” HCs (Edqvist et al., 2008; Tanabe et al., 2006). Therefore, this model is more representative of Ptf1a activity on HC subtype determination in vertebrates.

This study aimed to gain a better understanding of the molecular regulation underlying the Ptf1a activity during retinal development using the chick retina model. In this study, we showed that the forced expression of Ptf1a leads to a massive disorganization of the differentiated retina and changes in retinal cell representation that complement the retinal phenotype of *Ptf1a*-null mice: an increase of ACs and *all* HC subtypes and a decrease of ganglion and photoreceptor cells. Using this model, we identified several retinogenic factors that were rapidly regulated by Ptf1a overexpression and reported that ectopic Ptf1a strongly

downregulated *Atoh7* expression in the chick retina. Finally, our study demonstrated that the interaction between Ptf1a and Rbpj cofactors was required for Ptf1a activity in the developing retina.

MATERIALS AND METHODS

Animals

Gallus gallus white leghorn embryos were obtained from Haas (France). The animal experimentation was conducted in accordance with the Association for Research in Vision and Ophthalmology (ARVO) statement on the use of animals in Ophthalmic and Vision Research and a protocol approved by our local animal care committee.

DNA sequences

Chick genome sequences (V2.0 and V3.0) were obtained from The Genome Institute at Washington University (http://genome.wustl.edu/). The expressed sequence tags (accession numbers: BU487258 and BU347629) were ordered from Source Bioscience and sequenced (MWG-Operon). The alignments were performed using Basic Local Alignment Search Tool available at NCBI (http://blast.ncbi.nlm.nih.gov/) and VNTI software (Invitrogen).

Retroviral stock and plasmid production

The mouse *Ptf1a* was subcloned using specific CDS primers into the pDONR221 vector (Invitrogen) using BP clonase (Invitrogen). The Ptf1a mutants were generated using Polymerase Chain Reaction **(**PCR)-based mutagenesis. The pDONR221-Ptf1a plasmid was recombined in the presence of LR recombinase (Invitrogen) into either RCAS-BP(A)-NHY, which allowed for the fusion of a HA-tag with the N-terminal part of the Ptf1a protein (gift from Dr. Loftus) or the pCIG gateway vectors (Roger et al., 2006). The RCAS viral stocks

with titers > $1x10^8$ colony forming units per milliliter (cfu/ml) were prepared by transfecting DF1 cells with viral DNA constructs using FuGENE6 Reagent (Roche Diagnostics) (Yang, 2002). Viruses were concentrated by centrifugation using 100K Centrifugal Filters Amicon Ultra (Millipore). All embryos were injected into the right optic vesicle at embryonic day 2 (E2). The openings in the eggs were sealed with scotch tape and further incubated at 37.5°C. Parental RCAS-BP(A) viruses (Hughes et al., 1987) served as controls in the viral infection experiments.

Cryosection

The eyes were fixed in 4% paraformaldehyde (PFA) and incubated in 30% sucrose (Sigma) in phosphate-buffered saline (PBS) overnight followed by 1 hour incubation at 37°C in PGS (PBS, 7.5% gelatin (Sigma), and 10% sucrose). Eyes were embedded in PGS, frozen at -50°C in isopentane and stored at -80°C. Ten micrometer-thick cryosections were collected.

Cell dissociation

The retinas were collected in HBSS without Ca^{2+}/Mg^{2+}, trypsinized (1 mg/ml) (Sigma) and incubated for 10 minutes at 37°C. The digestion was stopped with HBSS with Ca^{2+}/Mg^{2+} containing trypsin inhibitor (Sigma) (1 mg/ml), and the cells were mechanically dissociated in the presence of DNaseI (Sigma) (0.1 mg/ml). For flow cytometry, the suspended cells were washed with PBS, fixed for 15 minutes with 2% PFA at room temperature (RT) and washed in PBS before immunostaining. For the manual counting, $1x10^5$ cells/ml were seeded on Poly-L-Lysine (Sigma) coated plates. After two hours, adherent cells were fixed 10 minutes with 2% PFA at RT before immunostaining.

Antibodies

Mouse anti-gag (3c2), anti-Ap2α (3B5), anti-Islet1 (39.4D5), anti-Lim1/2 (4F2), and anti-Visinin (7G4) antibodies were purchased from the Developmental Studies Hybridoma Bank. Mouse anti-Brn3a (MAB1585), mouse anti-Glutamine Synthetase (MAB302), mouse anti-Prox1 (MAB5652), and rabbit anti-PhosphoHistone3 (07-145) antibodies were obtained from Millipore, rabbit anti-gag (p27) from Charles River**,** rabbit anti-Protein Kinase Cα (PKCα) (Sc-208) from Santa Cruz, and rabbit anti-Prox1 (DP3501P) from Acris. The rabbit anti-Ptf1a antibody was a gift from Dr. Edlund (Umeå University), and the rabbit anti-TrkA was a gift from Pr. Lefcort (Montana State University). Primary antibodies were detected using AlexaFluor488-, AlexaFluor594-, AlexaFluor633- (Invitrogen) or Phycoerythrine (PE)- (Beckman Coulter) conjugated goat antibodies.

Immunostaining and *in situ* hybridization

Immunostaining was performed as previously described (Roger et al., 2006). Retinal section counterstaining was performed with 4',6'-diamidino-2-phenylindole (DAPI) (1:1200). Apoptotic cells were detected by terminal deoxynucleotidyl transferase (TdT)-mediated dUTP nick end labeling (TUNEL) labeling using the In Situ Cell Death Detection Kit (Roche Diagnostics). For S-phase cell labeling, 5 µg (E7 embryos) or 10 µg (E9 embryos) of 5-ethynyl-2'-deoxyuridine (EdU) were injected into the intravitreal space two hours before being sacrificed. The Click iT^{TM} EdU Imaging kit (Invitrogen) was used to visualize EdU-positive cells.

Digoxigenin-labeled *Rbpj* and *cAtoh7* probes were generated by cloning template DNA (the full length coding sequence of *cAtoh7* and the *cRbpj* coding sequence from 123 to 873 bp) into pCRII-TOPO vector (Invitrogen). *In situ* hybridization was performed as previously described (Roger et al., 2006).

Images were captured with a DM5500 microscope (Leica) equipped with an ORCA ER Hamamatsu camera or a LSM710 confocal microscope (Zeiss) and analyzed with MetaMorph software (Molecular Devices).

Flow cytometry and cell sorting

Dissociated cells were incubated in blocking buffer (PBS, 10% fetal calf serum (FCS), 2% goat serum, and 0.1% saponin) one hour at RT. Primary antibodies were diluted in blocking buffer, applied two hours at RT, and washed. The cell pellets were then incubated for one hour with 5 µl of PE- and/or AlexaFluor633-conjugated secondary antibodies (1:10) at RT. The data were collected using an LSRII cytometer (BD Biosciences) and analyzed using BD FACS DIVA software. For cell sorting, a total of $1x10^5$ GFP-positive cells were collected in lysis buffer for RNA extraction using Vantage Sorter (BD Biosciences).

Electroporation

The eyes were collected at E5, and the pigmented epithelium was removed from the retina. Whole retinas were positioned in an electroporation chamber (CUY520P5, Sonidel, Napagene, Japan) filled with PBS with Ca^{2+}/Mg^{2+} containing plasmids (0.5 µg/µl). Electroporation was performed using a CUY215C square wave generator (Sonidel) and consisted of 5 pulses at 30 V with 50 ms duration, 1 second interval and repeated twice. Whole retinas were then cultured as floating explants at 37°C in DMEM, 10% FCS, and 1% Penicillin/Streptomycin. For confocal microscopy, the retinas were fixed 20 minutes in 4% PFA and rinsed for 24 hours in PBS. For inclusion, the fixed retinas were cryoprotected and embedded in PGS.

RNA isolation, reverse-transcription and quantitative PCR.

Total RNA was extracted using the Nucleospin RNAII Kit (Macherey Nagel). Retrotranscription was performed as described previously (Roger et al., 2006). Real-time PCR was performed using 7300 Real-Time PCR System (Applied Biosystems) in a 20 µl final volume with Power SYBR Green PCR Master Mix (Applied Biosystems) and 0.25 µM primers. All samples were run in triplicate. Primers used for real-time PCR analysis are listed in Table S1 (See Supplementary Materials).

Cell fractionation

Protein extracts were collected in hypotonic buffer (20 mM HEPES pH 7.9, 1 mM Na_3VO_4, 1 mM NaGlycerophoshate, 5 mM EDTA pH 7.5, 1 mM EGTA pH 7.5, 1 mM DTT, and protease inhibitors (Calbiochem, Merck4Biosciences)) plus 0.2% Nonidet P-40, incubated on ice for 15 minutes and centrifuged (20 seconds at 16000 g). For nuclear extracts, pellets were resuspended in saline buffer (120 mM NaCl and 20% glycerol in hypotonic buffer) supplemented with protease inhibitor cocktail, incubated for 30 minutes at 4°C and centrifuged for 20 minutes at 16000 g to collect the supernatant. For cytosolic extracts, NaCl (120 mM) was added to the supernatant of the first centrifugation, and the extract was centrifuged for 20 minutes at 16000 g to remove debris. Glycerol (10%) was then added to the supernatant.

Western Blotting

Western Blotting was conducted as described previously (Roger et al., 2006) using the following primary antibodies: mouse anti-HA (MMS 101R, Covance), goat anti-LaminB (sc-6216, Santa Cruz), mouse anti-Actin (Sigma), goat anti-Ptf1a (ab62818, Abcam), and rat anti-Rbpj (T6719, Institute of Immunology, Tokyo, Japan).

Co-immunoprecipitation

Infected DF1 cells were lysed in immunoprecipitation buffer (50 mM Tris/HCl pH 8.0, 120 mM NaCl, 0.5% Nonidet P-40, and protease inhibitors) (Rodolosse et al., 2009). The lysates were incubated overnight and centrifuged for 20 minutes at 16000 g. Protein extracts (250 µg) were incubated with anti-HA antibody (Covance, 1/100) for 2 hours at RT to immunoprecipitate the HA-tagged proteins. The immune complex was then captured by incubating for 2 hours at RT with 40 µl of Protein-G Sepharose beads (Fast Flow, GE Healthcare). The complexes were pelleted by gentle centrifugation, washed four times with immunoprecipitation buffer and eluted in the loading buffer before western blotting.

Statistical analyses

The quantifications are expressed as the mean ± standard error of the mean (s.e.m). Analyses were conducted using the Student's t-test assuming equal variances (two groups) or one-way analysis of variance followed by Tukey's multiple comparison tests (three or more groups) using Prism 5.0 (Graphpad software). (*) $p<0.05$, (**) $p<0.01$, (***) $p<0.001$, (ns) not significant. p_{anova}, p-value of the one-way analysis of variance; p_{Tukey}, p-value of the Tukey post-hoc test.

RESULTS

Forced expression of Ptf1a results in a loss of retinal lamination.

The Ptf1a spatiotemporal expression pattern has been studied during retinogenesis (Boije et al., 2008; Fujitani et al., 2006; Nakhai et al., 2007). *Ptf1a* mRNA was detected from embryonic day 3 (E3) to E15 in the developing chick retina. Early, it is expressed in the inner neuroblastic layer (NBL) and then becomes restricted to the inner nuclear layer (INL) (Boije et al., 2008). To gain insight into the function of Ptf1a during chick retinal development, a replication-competent retrovirus, RCAS, was used to drive ectopic and overexpression of

Ptf1a in the retina. The chick *Ptf1a* gene sequence is not fully known. We have characterized its C-terminal using the available information at The Genome Institute and two ESTs. It contains the highly conserved bHLH DNA-binding and Rbpj/Rbpjl-interaction domains (Beres et al., 2006) (Fig. S1). However, the N-terminal of the chick *Ptf1a* gene has remained uncharacterized in recent chicken genome assemblies. In contrast, the mouse *Ptf1a* sequence is fully known, and the Rbpj/Rbpjl-interaction domains have been extensively studied (Beres et al., 2006). Moreover, previous studies have reported that mouse Ptf1a blocks the differentiation of dIL_B excitatory neurons and promotes dIL_A inhibitory neuron specification in the chick spinal cord, a phenotype that was consistent with *Ptf1a* loss of function studies in mouse (Glasgow et al., 2005; Hori et al., 2008; Mizuguchi et al., 2006; Wildner et al., 2006). These results suggest a conserved activity of mouse Ptf1a in avian and rodent models. Therefore, the mouse *Ptf1a* cDNA was chosen to allow for misexpression experiments of Ptf1a in the chick retina and for genetic manipulations of the *Ptf1a* coding sequence. Effective wild type Ptf1a protein mis/overexpression from RCAS-HA-Ptf1a (RCAS-Ptf1a) was verified by western blotting for the HA-tagged proteins in DF1 cells (Fig. 1A) and by immunohistochemistry in E9 retinas (Fig. 1D). In the chick retina, viral injections resulted in a widespread infection. Retinal patches infected with the different RCAS viruses and infected retinal dissociated cells could be detected using either the p27 or 3c2 anti-gag antibodies (Fig. 1C,E).

During any developmental stage, the plexiform and nuclear layers had formed properly in the empty-RCAS (RCAS) control infected patches (Fig. 1F-G,J-K,N-O). At E7, no major structural defects were observed in the RCAS-Ptf1a-infected patches other than the presence of a thicker retina and a decreased cell density (Fig. 1H-I). In contrast, at E9 (Fig. 1L-M) and, more extensively, at E12 (Fig. 1P-Q), the lamination of the RCAS-Ptf1a-infected patches was severely disturbed with disorganized plexiform and nuclear layers. No changes in

the retinal structure were observed outside of the RCAS-Ptf1a-infected areas (data not shown).

Forced expression of Ptf1a affects progenitor cell proliferation and migration.

These defects in retinal structure and lamination might arise from disturbed migration or modification of the cell cycle. Therefore, S-phase cells were pulse-labeled with 5-ethynyl-2'-deoxyuridine (EdU), and mitotically active progenitors were immunostained using a Phospho-Histone3 (P-H3) antibody. At E7, in the control retinas, EdU-positive cells were located in the NBL (Fig. 2A), whereas P-H3 positive cells were primarily found in the ventricular side (Fig. 2E), which was consistent with interkinetic nuclear movements (IKNM) of progenitor nuclei and free-cell migration (Baye and Link, 2008; Boije et al., 2009; Hinds and Hinds, 1979). P-H3-positive (Fig. 2F) and numerous EdU-positive cells (Fig. 2B) were detected within the RCAS-Ptf1a-infected patches at E7. The EdU-positive cells were mislocalized in the ventricular half of the retina (Fig. 2B), and an increased number of ectopic P-H3 positive cells were detected in the NBL and in the vitreal side of the RCAS-Ptf1a-infected patches (Fig. 2F, arrows and Fig. S2). These results suggest that the movement of progenitors was altered in the RCAS-Ptf1a-infected retina at E7 and might partially account for the observed structural defects.

The EdU-positive and P-H3-positive cells were scored using flow cytometry. The percentage of EdU-positive cells among the infected cells was normalized by the percentage of EdU-positive cells among non-infected cells. At E7, the number of EdU-positive cells was significantly decreased following the forced expression of Ptf1a ($p=0.031$) (Fig. 2I). At E9, fewer EdU- ($p=0.001$) (Fig. 2D) and P-H3-positive cells (Fig. 2H) ($0.14 \pm 0.04\%$, s.e.m, in the RCAS-infected cells and $0.02 \pm 0.01\%$, s.e.m, in the RCAS-Ptf1a-infected cells, $p=0.0178$) were detected after Ptf1a mis/overexpression (Fig. 2I,J). Together, these findings

suggest that the forced expression of Ptf1a induced progenitors to withdraw from the cell cycle.

Ptf1a mis/overexpression is sufficient to induce a change in retinal cell type representation.

To investigate whether the structural and cell cycle changes were paired with alterations in the proportion of major retinal cell types, using immunocytochemistry, we analyzed the markers of the different cell classes in the infected areas of E12 retinas, the age when most cells have initiated their differentiation. Concomitantly, the number of ACs, HCs and photoreceptor cells among the gag-positive infected cells was scored by flow cytometry. At E12, immunoreactivity for Ap2α was found in most AC nuclei in the INL (Fig. 3K) (Edqvist et al., 2006; Fischer et al., 2007). Prox1 strongly labeled HCs and a small subset of ACs (Fig. 3P). The forced expression of Ptf1a induced a three-fold increase of Ap2α-positive cells compared to control cells (22.7 ± 2.2% in the RCAS-infected population and 63.0 ± 12.9% in the RCAS-Ptf1a-infected population, n=5) and a two-fold increase of Prox1-positive cells (18.0 ± 1.3% in the RCAS-infected population and 32.6 ± 4.7% in the RCAS-Ptf1a-infected population, n=5) (Fig. 3L,Q,W). Conversely, Brn3a labeling for ganglion cells was severely reduced in the RCAS-Ptf1a-infected patches (Fig. 3B), and the number of Visinin-positive photoreceptors was decreased from 17.7 ± 2.6% in the RCAS-infected cells to 4.2 ± 0.5% in the RCAS-Ptf1a-infected cells (n=5) (Fig. 3G,U-W). For late born retinal cell subtypes, the number of Glutamine Synthetase (GS)-positive Müller glial cells was significantly decreased from 3.2 ± 0.2% in the RCAS-infected cells to 1.8 ± 0.3% in the RCAS-Ptf1a-infected cells (p=0.0083, n=4) (Fig. S3B,E), but Protein Kinase Cα (PKCα) immunoreactivity for rod bipolar cells revealed no significant difference (1.8 ± 0.1%

among the RCAS-infected cells and 3.9 ± 0.8% among the RCAS-Ptf1a-infected cells, p=0.2651, n=4) (Fig. S3D,E).

Retinal lamination defects at E9 and later stages may result in a secondary alteration of cell type representation. Therefore, we conducted the same analysis prior to the structural defects, at E7. At this age, Ptf1a mis/overexpression also led to a significant increase of Prox1- (4.4 ± 0.3% among the RCAS-infected cells and 14.7 ± 1.5% among the RCAS-Ptf1a-infected cells, p=0.0004, n=4) (Fig. 4F,I) and Ap2α-positive cells (10.9 ± 0.1% among the RCAS-infected cells and 18.9 ± 1.2% among the RCAS-Ptf1a-infected cells, p=0.001, n=5) (Fig. 4H,I) at the expense of ganglion cells (Fig. 4B) and photoreceptor cells (10.2 ± 0.7% in the RCAS-infected retinas and 6.5 ± 0.4% in the RCAS-Ptf1a-infected retinas, p=0.0014, n=5) (Fig. 4D,I). These results indicated that the Ptf1a mis/overexpression effects on early-born retinal cell types occurred prior to the defects in retinal lamination and argued against the notion that the loss of photoreceptors and ganglion cells was secondary to the retinal lamination defects. Interestingly, a few Ap2α-positive cells (Fig. 4H) and the majority of Prox1-positive cells (Fig. 4F) were ectopically located in the vitreal side of the retina.

We performed TUNEL labeling to assess if the reduction of some cell subtypes could be due to early cell death. A significantly higher number of apoptotic cells, located throughout the entire thickness of the NBL, was detected in the RCAS-Ptf1a patches (43.3 ± 9.8 cells per area) compared to the patches infected with the control virus (8.5 ± 0.2 cells per area, n=3, p=0.0305) (Fig. 4J-L).

Ptf1a mis/overexpression is sufficient to induce all HC subtype specification.

Our results showed that Ptf1a mis/overexpression increased the size of the HC population. The chick HC population is composed of at least three HC subtypes that can be molecularly distinguished by the expression of Prox1, Lim1, Islet1, TrkA and GABA

(Edqvist et al., 2008; Fischer et al., 2007). All three subtypes express Prox1. The H1 subtype (50% of all HCs) has GABA, is Lim1-positive, Islet1-negative, and TrkA-negative. The H2 (approximately 10% of all HCs) also has GABA, is Lim1-negative, Islet1-positive but TrkA-negative, and the H3 (approximately 40% of all HCs) does not have GABA, is Lim1-negative and Islet1/TrkA double-positive. We first investigated the normal Ptf1a expression in the HC subtypes in the developing chick retina. The retina was analyzed with respect to Ptf1a, Prox1, Lim1 and Islet1 immunoreactivity in E6.5 retinas when HCs migrated bi-directionally and, in E9, E12 and E16 retinas when the HC layer (HCL) was established (Boije et al., 2009; Edqvist and Hallbook, 2004). At E6.5, after the onset of Prox1 expression in HCs, 31 ± 5% (n=3) of the Ptf1a-immunoreactive cells were also Prox1-positive (Fig. 5A). The Ptf1a/Prox1 double-positive cells were localized on the vitreal side of the retina but also scattered in the prospective INL, which was consistent with the location of migrating HCs at this age. At E9, all Ptf1a/Prox1 double-positive cells were located in the developing HCL. Of the Prox1-positive cells in the HCL, 64 ± 5% (n=3) were Ptf1a-positive HCs (Fig. 5B). This result implies that not all HCs expressed Ptf1a at this age. The Lim1-positive cells were Ptf1a-positive, and this overlap was found at both E9 (96 ± 1%, n=3) in the HCL and at earlier ages on the vitreal side (Fig. 5E,F). In contrast, only a few Ptf1a/Islet1 double-positive cells could be seen at E6.5 and at E9 (5 ± 0.6%, n=3) (Fig. 5I,J).

To assess whether Ptf1a was able to direct the development of all HC subtypes, we next analyzed the presence of HC subtype markers in the RCAS-Ptf1a-infected patches. At E7, an accumulation of Prox1/Lim1 double-positive and Prox1/Islet1 double-positive cells (Fig. 6B,D) were found in the normal location of the GCL in the RCAS-Ptf1a-infected patches compared to the control patches, suggesting that both the H1 and H3 subtypes had been generated following Ptf1a mis/overexpression. These results were strengthened by the TrkA immunoreactivity of Islet1-positive cells in the RCAS-Ptf1a-infected areas (Fig. 6F).

Furthermore, the accumulation of some HCs in the vitreal side suggested that HC migration was either arrested or delayed by Ptf1a mis/overexpression. These results were similar at E9 when all HCs had normally migrated back to the HCL. Supernumerary Prox1/Lim1 double-positive (Fig. 6H), Prox1/Islet1 double-positive (Fig. 6J), and Islet1/TrkA double-positive cells (Fig. 6L) were observed in the RCAS-Ptf1a-infected retinas. Islet1-positive and TrkA-negative cells were found within the clusters of Prox1-positive cells of the RCAS-Ptf1a-infected patches (Fig. 6l, arrows), suggesting the presence of H2 HCs. Moreover, TrkA and Lim1 were never expressed in the same cell, indicating that H1 and H3 HCs were correctly specified (Fig. 6N). We found that the proportion of non-GABAergic TrkA-positive cells among the Prox1-positive HCs decreased significantly from 43.3 ± 1.9% in the RCAS-infected patches to 27.1 ± 2.8% in the RCAS-Ptf1a-infected areas (p=0.0007), whereas a slight, but not significant, increase of Lim1-positive HCs was observed (51.9 ± 2.2% in the RCAS-infected patches and 58.9 ± 2.1% in the RCAS-Ptf1a-infected patches, p=0.0898) (Fig. 6O). Moreover, the back-migration of ectopic HCs to the HCL was inhibited, and ectopic HCs remained on the vitreal side of the E9 RCAS-Ptf1a-infected retinas.

Ptf1a overexpression induces changes in retinogenic factor expression.

To gain knowledge about the molecular mechanisms underlying the changes in retinal cell specification, we studied early changes in the expression of a selected set of genes involved in retinal differentiation. The E5 whole chick retinas were electroporated *ex vivo* with pCIG-Ptf1a-GFP plasmids, which drive the green fluorescent protein (GFP) expression (Roger et al., 2006) (Fig. 7A). The GFP-positive cells were isolated by fluorescence activated cell sorting as early as 36 hours after electroporation to study changes in gene expression that were as independent as possible from cell differentiation. The empty pCIG-GFP plasmids were used as controls. First, our quantification demonstrated that electroporation of pCIG-

Ptf1a in the chick retinas resulted in a strong expression of mouse *Ptf1a* mRNA, compared to the reference level (the non-specific amplification in pCIG-electroporated retinal cells) (Fig. 7B). Surprisingly, endogenous chick *Ptf1a* mRNA levels were significantly decreased in the mouse Ptf1a-overexpressing cells (p=0.0002) (Fig. 7B). No effects were observed on either *Ngn2*, a direct target of Ptf1a in the spinal cord and the cerebellum (Henke et al., 2009), or *Sox2*. We found that *Pax6* and *Ap2α*, coding for two transcription factors highly expressed in ACs (Belecky-Adams et al., 1997; de Melo et al., 2003; Edqvist et al., 2006), were upregulated in Ptf1a-overexpressing cells (p=0.009) (Fig. 7B). A significant 2.6-fold increase of *NeuroAB* mRNA, a transcription factor suggested to be involved in GABAergic AC development (Ohkawara et al., 2004), was also observed in Ptf1a-overexpressing cells (p=0.0167). Interestingly, the expression levels of *Ascl1*, a pro-amacrine transcription factor in chick retina (Mao et al., 2009), was downregulated (p=0.0037), suggesting that Ptf1a might act downstream of Ascl1 and inhibit its expression in the retina as described in the spinal cord (Hori et al., 2008). The expression level of *Otx2*, a key regulatory gene for photoreceptor development (Nishida et al., 2003), was decreased by 2.5-fold in Ptf1a-overexpressing cells (p=0.0076), and *Atoh7*, a transcription factor involved in ganglion cell specification (Liu et al., 2001; Matter-Sadzinski et al., 2005), was strongly repressed by 6.4-fold by Ptf1a overexpression (p=0.0071) (Fig. 7B). Furthermore, *Atoh7* mRNA was nearly undetectable by *in situ* hybridization in RCAS-Ptf1a-infected patches (Fig. S5C). Consistently, *ex vivo*, ectopic Ptf1a downregulated the activity of the chick *Atoh7* promoter. Indeed, a significant decrease in the number of GFP-positive cells was observed in retinas co-electroporated with RCAS-Ptf1a and pAtoh7-GFP, a plasmid that drives GFP expression under the control of the chick *Atoh7* promoter, compared to RCAS and pAtoh7-GFP co-electroporated retinas (Fig. S5E,F,H, $p_{anova}=0.001$, $p_{tukey}<0.01$).

We further focused our analysis on transcription factors involved in HC genesis. The mRNA levels of *Neurod4* (Fig. 7B) and *Prox1* (Fig. 7C), two factors involved in HC development (Dyer et al., 2003; Inoue et al., 2002), were not altered, whereas *Lim1*, which is necessary for H1 specification in the chick retina (Suga et al., 2009), was induced following Ptf1a overexpression (Fig. 7C). Foxn4 is upstream of Ptf1a during AC/HC specification in mouse retina (Fujitani et al., 2006; Li et al., 2004). Interestingly, Ptf1a overexpression induced a two-fold decrease of *Foxn4* expression levels (p=0.0030) (Fig. 7C). To investigate whether Foxn4 conversely regulates *Ptf1a* in the chick retina, we electroporated E5 retinas with pCIG-Foxn4-GFP vectors (Fig. 7A). Foxn4 overexpression resulted in a significant increase in *Ptf1a* expression (p=0.0498) and *Lim1* and *Prox1* mRNA expression levels (Fig. 7C).

Ectopic Ptf1a requires its interaction with endogenous RBP-J

Ptf1a forms the PTF1 complex with any one of the E-proteins and Rbpj (PTF1-J) or Rbpjl (PTF1-L) (Beres et al., 2006). Ptf1a interacts with Rbpjl through its C1 domain and with Rbpj through its C2 and C1 domains (Fig. S4K). The C2 domain deletion was sufficient to abolish the formation of the PTF1-J complex (Beres et al., 2006). *In situ* hybridization revealed that *Rbpj* mRNA was expressed throughout the NBL at early stages and in the INL at later stages up to E12 (see Fig. S6A-J). Conversely, *Rbpjl* mRNA was neither detected during chick retinal development (data not shown) nor in mature retinas by quantitative PCR (Fig. S6K). To test the requirement for Rbpj proteins for Ptf1a activity in the chick retina, we generated Ptf1a-ΔC2 and Ptf1a-ΔC1ΔC2 (Ptf1a-ΔC12) mutant forms of Ptf1a that interact with E-proteins but are unable to interact with Rbpj (Beres et al., 2006) (Fig. S4L). The Ptf1a-ΔC2 and Ptf1a-ΔC12 proteins were expressed at levels equivalent to Ptf1a full-length proteins (Fig. S4N). Moreover, subcellular fractionation revealed that deletion of the C1 and C2 domains did not prevent Ptf1a-ΔC12 nuclear importation (Fig. S4O). The injection of RCAS-

Ptf1a-ΔC2 and RCAS-Ptf1a-ΔC12 in the optic cup did not lead to gross structural defects of the retina (Fig. 3 and Fig. S4E-H). However, the outer plexiform and nuclear layers were disrupted with rosette-like structures (Fig. 3H,I). Early-born cell types were analyzed by immunochemistry and flow cytometry in the RCAS-Ptf1a-ΔC2- and RCAS-Ptf1a -ΔC12-infected population of E12 retinas, but no alteration of the cell type distribution was observed following the forced expression of these two Ptf1a mutant forms (Fig. 3C-D,H-I,M-N,R-S,W). The requirement of Rbpj-Ptf1a interaction for gene regulation downstream of ectopic Ptf1a was assessed by evaluating the ability of ectopic Ptf1a-ΔC12 to regulate the *Atoh7* promoter activity. Co-electroporation of pAtoh7-GFP with the RCAS-Ptf1a-ΔC12 plasmids did not decrease the number of GFP-positive cells compared to co-electroporation with the control RCAS vectors (Fig. S5G,H).

Ectopic Ptf1a activity is independent from Rbpj pool depletion

Rbpj is a major downstream effector of the Notch pathway. Previous studies have suggested that the Ptf1a activity might be downregulated by sequestering Rbpj from Ptf1a (Cras-Meneur et al., 2009) following Notch activation. Therefore, we examined if ectopic Ptf1a might function in the chick retina by conversely sequestering Rbpj. We generated a Ptf1a-Δbasic mutant where the highly conserved RER-R amino acids (168-172) (Fig. S4L,M) in the basic domain were replaced by AVA-A. These mutations were shown to abolish MyoD and bHLHa15/Mist1 bHLH transcription factor binding to DNA (Lemercier et al., 1998; Skowronska-Krawczyk et al., 2005). The Ptf1a-Δbasic protein was still imported into the nucleus (See Fig. S4O) and retained its ability to interact with Rbpj (See Fig. S4P). The *in vitro* reporter assay confirmed that the transcriptional activity of Ptf1a-Δbasic was strongly decreased (data not shown). No alteration of retinal structure and cell type representation (Fig. 3E,J,O,T and Fig. S4I-J) was detected within the E12 RCAS-Ptf1a-Δbasic-infected patches.

This result argues against the hypothesis that the activity of wild-type ectopic Ptf1a might be completely mediated by a disruption of Rbpj function.

DISCUSSION

Our study demonstrated that Ptf1a was sufficient to affect the chick retinal cell composition in an Rbpj-dependent manner. Our "candidate-gene" approach showed that Ptf1a overexpression selectively upregulated *NeuroAB, Ap2α* and *Lim1* while it downregulated *Otx2* and *Atoh7*. This study provides a new molecular basis for Ptf1a activity in specifying the ACs and all HC subtypes and inhibiting photoreceptor and ganglion cell genesis.

Cellular and molecular mechanisms underlying ectopic Ptf1a activity during chick retinal development.

Several hypotheses may explain the changes in cell type representation induced by Ptf1a.

First, cell proliferation defects may change the final retinal cell composition. Indeed, early cell cycle exit has been shown to favor early-born retinal cell types. Conversely, late cell cycle exit biases progenitor cells toward later neuronal fates (Austin et al., 1995; Dorsky et al., 1997; Henrique et al., 1997; Jadhav et al., 2006; Livesey and Cepko, 2001; Nelson et al., 2007; Ohnuma et al., 2002; Silva et al., 2003; Yaron et al., 2006). We found that the forced expression of Ptf1a in the chick retina induced a premature cell-cycle exit, but led to a dramatic decrease of early-born ganglion and cone photoreceptor cells. Thus, it is unlikely that cell proliferation defects alone account for the effect of ectopic Ptf1a activity in chick retinogenesis. How Ptf1a induced cell cycle withdrawal remains to be defined. The cell cycle exit could be linked to the defects in the IKNM of retinal progenitors observed following Ptf1a mis/overexpression. Indeed, in the chick retina, pharmacological perturbation of IKNM

was shown to promote premature neurogenesis (Murciano et al., 2002) through a reduction of Notch-mediated lateral inhibition (Del Bene et al., 2008; Murciano et al., 2002). Consistent with this model, the expression of Hes5, a target of the Notch pathway in the retina (Nelson et al., 2006), was significantly decreased in electroporated Ptf1a-overexpressing cells (data not shown). Moreover, the expression level of cyclin D1 that is required for RPC proliferation (Fantl et al., 1995; Godbout and Andison, 1996; Sicinski et al., 1995) was also significantly downregulated in Ptf1a-overexpressing cells (data not shown), suggesting that ectopic Ptf1a might regulate the core of the cell cycle machinery.

Second, Ptf1a might bias progenitor cells toward the AC and HC fates. We found that the expression of *Atoh7* (Brown et al., 2001; Wang et al., 2001) and *Otx2* (Nishida et al., 2003), which specify ganglion cells and photoreceptors, respectively, were inhibited in cells that overexpressed Ptf1a. In contrast, *Lim1*, involved in HC specification (Suga et al., 2009), and *NeuroAB*, which is presumably involved in AC genesis (Ohkawara et al., 2004), were upregulated. These transcriptional regulations support a mechanism where ectopic Ptf1a might act cell-autonomously to drive retinal progenitors toward the AC and HC fates at the expense of ganglion cells and photoreceptors by regulating their transcriptional program. The effects of ectopic Ptf1a on cell fate might also be influenced by cell proliferation regulation. Indeed, early cell cycle exit was shown to enhance the activity of proneural factors (Atoh7, Ngn1, and Neurod4) that promote early cell fates (Ohnuma et al., 2002). Recently, the majority of Ptf1a-expressing cells were found to originate from Atoh7-positive progenitor cells, and Ptf1a expression drove their differentiation toward ACs/HCs at the expense of ganglion cells in the zebrafish retina (Jusuf et al., 2011). Our overexpression study showed that ectopic Ptf1a was a negative regulator of *Atoh7*. Therefore, it would be interesting to assess whether *endogenous* Ptf1a, which is turned on after Atoh7 in the Atoh7-positive

lineage, is able to downregulate Atoh7 expression during retinogenesis, how it might regulate *Atoh7*, and if this regulation is involved in the fate switch toward ACs/HCs.

Third, Ptf1a might also selectively induce the death of ganglion and photoreceptor cells, modifying the cell representation in favor of ACs/HCs. The number of apoptotic cells was increased in Ptf1a-infected retinas at E7, but the precise determination of their identity was difficult to assess because many apoptotic cells have lost their differentiation markers. To our knowledge, no report has demonstrated a direct induction of cell death either by Ptf1a or by the misexpression of transcription factors without apoptotic regulatory properties. Dullin et al. (Dullin et al., 2007) did not detect any apoptosis induction following Ptf1a overexpression in *Xenopus* retinas, suggesting that Ptf1a has no pro-apoptotic function *per se*. Secondary cell death is a common feature of transcription factor gain- and loss-of-functions and has often been associated with defects in cell trans-commitment in the retina (Fujitani et al., 2006; Mao et al., 2009; Qiu et al., 2008; Zheng et al., 2009). Therefore, the increase in cell death is likely a secondary event that occurs following the late re-specification of already committed precursors. Alternatively, a lack of crucial trophic support and inappropriate cell-cell interactions may lead to the elimination of prematurely differentiated cells.

Transcriptional regulation upstream and downstream of Ptf1a

Our results showed that Foxn4 upregulated *Prox1*, *Lim1* and *Ptf1a* in the chick retina, suggesting that Foxn4 might be sufficient to induce HC fate in the developing chick retina, which is in contrast to mice (Li et al., 2004). Together with the upregulation of endogenous *Ptf1a* by Foxn4, these data confirm that Ptf1a functions downstream of Foxn4 in the transcriptional cascade leading to HC specification as proposed in mice (Fujitani et al., 2006). Interestingly, we discovered that Ptf1a downregulated *Foxn4*, indicating that Ptf1a would be required to finely regulate Foxn4 expression in HC and AC precursors. In line with this

hypothesis, Li et al. reported that in *Foxn4*^{LacZ} knock-in mice, β−galactosidase (LacZ) expression was upregulated and persisted longer than in wild type retinas (Li et al., 2004). This *Foxn4* locus deregulation could result, at least partially, from the loss of Ptf1a expression in *Foxn4*$^{-/-}$ mice (Fujitani et al., 2006).

An increase in photoreceptor cells was reported in addition to the decrease of ACs/HCs following *Foxn4* and *Ptf1a* inactivation (Dong et al., 2008; Dullin et al., 2007; Fujitani et al., 2006; Li et al., 2004; Nakhai et al., 2007). Consistently, our misexpression study demonstrated that Ptf1a inhibited photoreceptor cell production and decreased *Otx2* expression. Inversely, the loss of *Otx2* in the mouse retina decreased the number of photoreceptors in favor of ACs (Nishida et al., 2003). These gain- and loss-of-function studies highlight a possible connection between the production of HCs/ACs on the one hand and photoreceptors and ganglion cells on the other. This balance may rely, to some extent, on Notch-mediated lateral inhibition. Notch signaling was shown to specifically inhibit mouse photoreceptor specification (Jadhav et al., 2006; Yaron et al., 2006). In various structures of the central nervous system, Ascl1 and Foxn4 have been implicated in the regulation of the Delta-like/Notch signaling pathway. Notably, in the ventral spinal cord, Foxn4 functions upstream of Ascl1, Delta-like and Notch expression to regulate the diversification of excitatory and inhibitory V2 cells by lateral inhibition (Del Barrio et al., 2007). In the retina (Nelson et al., 2009; Nelson and Reh, 2008) and mouse dorsal spinal cord (Mizuguchi et al., 2006), Ascl1 activates Delta-like and Ptf1a expression. Thus, similar to the spinal cord, Foxn4 and/or Ascl1 might initiate lateral inhibition among a subset of retinal progenitors. These factors would then be required to sustain Notch signaling in AC/HC precursors that were activated by Delta-expressing neighboring cells that were prone to differentiate as photoreceptor cells. Ascl1 and Foxn4 expression would also contribute to turning off the photoreceptor and ganglion cell specification programs in AC/HC precursors through Ptf1a

activation. Further studies will be needed to determine to what extent Foxn4 and Ascl1 function together to regulate Notch signaling and Ptf1a expression in the chick retina. Ptf1a alone might not sustain Notch signaling because Hes5 was downregulated in Ptf1a-overexpressing cells (data not shown).

Surprisingly, endogenous chick Ptf1a mRNA levels were significantly decreased in mouse Ptf1a-overexpressing cells. These results were in contrast with the positive autoregulation of Ptf1a that occurs in the pancreas, spinal cord and cerebellum (Masui et al., 2008; Meredith et al., 2009). Recently, Jusuf et al. (Jusuf et al., 2011) reported that a feedback loop originating from HCs/ACs operated to limit the number of cells initiating Ptf1a expression in the zebrafish retina. Thus, supernumerary ACs/HCs might regulate the expression of pro-amacrine factors, such as Foxn4 and Ptf1a, in autocrine or paracrine feedback loops. Alternatively, our results demonstrated that *Foxn4* was downregulated in mouse Ptf1a-overexpressing cells and that Foxn4 activated endogenous chick *Ptf1a*. Chick *Ptf1a* expression would not be triggered in mouse Ptf1a-overexpressing cells as a result of the absence of its upstream activator, Foxn4.

PTF1-J complex during retinogenesis

Previous studies have demonstrated that the Ptf1a/Rbpj/E-protein (PTF1-J) complex is the functional endogenous PTF1 complex required for GABAergic cell specification in mouse cerebellum and spinal cord (Hori et al., 2008). Nonetheless, the formation of this functional trimeric complex during retinogenesis has not yet been assessed. In this study, we showed that the loss of the Rbpj-binding domains within the Ptf1a protein was sufficient to abolish the Ptf1a effects on chick retinal cell differentiation, indicating that *ectopic* Ptf1a was dependent on the Rbpj cofactors in the chick retina.

Does the *endogenous* Ptf1a factor require Rbpj for the specification of ACs and HCs? Several points suggest that this functional interaction occurs. First, we showed that Rbpj was expressed in the retina during retinogenesis, notably in the INL (Fig. S6A-J). Second, recent conditional loss-of-function studies (Riesenberg et al., 2009; Zheng et al., 2009) reported that retinas null for *Rbpj* exhibited a phenotype that mimics some features of the *Ptf1a*-null retinas (Fujitani et al., 2006; Nakhai et al., 2007) and complement our gain-of-function study. Indeed, the loss of *Rbpj* in the retina induced an increase of ganglion cells together with an upregulation of *Atoh7* (Riesenberg et al., 2009; Zheng et al., 2009). Moreover, the loss of *Rbpj* in Chx10-positive retinal cells induced a significant decrease of ACs and HCs in P21 mouse retinas (Zheng et al., 2009). The ganglion cell increase was attributed to Notch3 signaling inhibition (Riesenberg et al., 2009). We found that the Ptf1a-Rbpj interaction was necessary to inhibit ganglion cell specification following Ptf1a overexpression. Based on our study, the increase in ganglion cell number in *Rbpj*-null mice might result from either Notch3 signaling inhibition or from endogenous PTF1-J complex inactivation. The increase of ACs/HCs was not observed following *Rbpj* inactivation in the alpha-positive peripheral retinal cells (Riesenberg et al., 2009).The discrepancies between the two conditional *Rbpj* knock-out mouse models might result from the inactivation of *Rbpj* in different progenitor pools or a genetic compensation by Rbpjl because Rbpj was shown to compensate for the loss of *Rbpjl* in the *Rbpjl*$^{-/-}$ mouse pancreas (Masui et al., 2010). They could also be due to the use of different amacrine cell markers.

It is noteworthy that, in humans, mutations of the Rbpj-interaction domain of Ptf1a protein caused optic nerve hypoplasy in addition to a cerebellar and pancreatic agenesis (Sellick et al., 2004). The same phenotype was reported in *Rbpj*-null mice where ectopic ganglion cells underwent cell death during late developmental stages. Even if the late specific cell death of the supernumerary ganglion cells remained to be assessed in *Ptf1a*-deficient

retina, this supports a highly conserved Ptf1a-Rbpj functional interaction during vertebrate retinal development.

Horizontal cell subtype specification by Ptf1a

It has been shown that Ptf1a is required to specify GABAergic neurons over glutamatergic neurons in the mouse dorsal spinal cord (Glasgow et al., 2005) and cerebellum (Hoshino et al., 2005). However, Ptf1a controls the specification of glutamatergic climbing fiber neurons of the inferior olivary nucleus (Yamada et al., 2007), suggesting that Ptf1a is a neuronal fate determinant in this structure. In the retina, two hypotheses were formulated: either Ptf1a is involved in all AC/HC specifications (Fujitani et al., 2006; Jusuf and Harris, 2009), or Ptf1a favors only the GABAergic cell subtypes (Dullin et al., 2007). We found in this study that the number of both H1 GABAergic cells (and probably H2 cells) and H3 non-GABAergic HCs were increased in the RCAS-Ptf1a-infected patches. Thus, Ptf1a is likely to act primarily as a general HC determination factor.

We detected only a few Islet1-positive HCs (H2 or H3 cells) that expressed endogenous Ptf1a during chick retinogenesis, which argues against a direct exclusion between Islet1 and Ptf1a. One hypothesis is that H3 HCs, which are the majority of the Lim1-negative and Islet1-positive, may not express Ptf1a and that the few Ptf1a/Islet1 double-positive cells in the HCL were H2 HCs. Alternatively, Ptf1a expression could be transiently required for the specification of H2/H3 cells and turned off at the onset of expression of H2 and H3 markers in the late-born Islet1-positive HCs (Edqvist et al., 2008). Consistent with this hypothesis in the zebrafish retina containing both Lim1-positive and Islet1-positive HC subtypes (Hallböök, unpublished), the knock-down of Ptf1a expression caused a decrease of Prox1/Islet1-positive HCs (Dong et al., 2008).

We found that Lim1-positive HCs expressed Ptf1a and that Ptf1a remained during bidirectional migration and once the cells stopped their migration in the HCL, indicating that Ptf1a might be involved in several steps of H1 cell specification/differentiation beyond its implication in all HC fate. In contrast, we found that Ptf1a downregulated Islet1 expression, suggesting that Ptf1a should be turned off for Islet1 to be expressed (data not shown). Therefore, secondary to the specification for all HCs, differential regulation of Ptf1a expression in the HC subtypes (sustained expression in H1 and downregulation in H2/H3) might be necessary to achieve their proper differentiation. In the context of forced and persistent Ptf1a expression, this regulation might fail and result in a decrease of the H3 proportion among HCs.

Acknowledgments: We thank Pr. Lefcort for the anti-TrkA antibody, Pr. Edlund for the anti-Ptf1a antibody, Pr. Real for the Ptf1aK200R construct and Pr. Loftus for the RCAS-BP(A)-NHY plasmid. We are grateful to Prs. Martinerie, Laurent and Chiodini for their helpful support. We acknowledge Drs. Sadzinski-Matter, Thomasseau and Sandlung for technical assistance. This work was financed by INSERM, Retina France, EU (LSHG-CT-2005-512036, ERC-StG-210345), French ANR (ANR-Geno-031-03, ANR-08-MNPS-003), Swedish Research Council, Swedish SSMF and SSF.

REFERENCES

Austin, C. P., Feldman, D. E., Ida, J. A., Jr., Cepko, C. L., 1995. Vertebrate retinal ganglion cells are selected from competent progenitors by the action of Notch. Development. 121**,** 3637-50.

Baye, L. M., Link, B. A., 2008. Nuclear migration during retinal development. Brain Res. 1192**,** 29-36.

Belecky-Adams, T., Tomarev, S., Li, H. S., Ploder, L., McInnes, R. R., Sundin, O., Adler, R., 1997. Pax-6, Prox 1, and Chx10 homeobox gene expression correlates with phenotypic fate of retinal precursor cells. Invest Ophthalmol Vis Sci. 38**,** 1293-303.

Beres, T. M., Masui, T., Swift, G. H., Shi, L., Henke, R. M., MacDonald, R. J., 2006. PTF1 is an organ-specific and Notch-independent basic helix-loop-helix complex containing the mammalian Suppressor of Hairless (RBP-J) or its paralogue, RBP-L. Mol Cell Biol. 26**,** 117-30.

Boije, H., Edqvist, P. H., Hallbook, F., 2008. Temporal and spatial expression of transcription factors FoxN4, Ptf1a, Prox1, Isl1 and Lim1 mRNA in the developing chick retina. Gene Expr Patterns. 8**,** 117-23.

Boije, H., Edqvist, P. H., Hallbook, F., 2009. Horizontal cell progenitors arrest in G2-phase and undergo terminal mitosis on the vitreal side of the chick retina. Dev Biol. 330**,** 105-13.

Brown, N. L., Patel, S., Brzezinski, J., Glaser, T., 2001. Math5 is required for retinal ganglion cell and optic nerve formation. Development. 128**,** 2497-508.

Cras-Meneur, C., Li, L., Kopan, R., Permutt, M. A., 2009. Presenilins, Notch dose control the fate of pancreatic endocrine progenitors during a narrow developmental window. Genes Dev. 23**,** 2088-101.

de Melo, J., Qiu, X., Du, G., Cristante, L., Eisenstat, D. D., 2003. Dlx1, Dlx2, Pax6, Brn3b, and Chx10 homeobox gene expression defines the retinal ganglion and inner nuclear layers of the developing and adult mouse retina. J Comp Neurol. 461**,** 187-204.

Del Barrio, M. G., Taveira-Marques, R., Muroyama, Y., Yuk, D. I., Li, S., Wines-Samuelson, M., Shen, J., Smith, H. K., Xiang, M., Rowitch, D., Richardson, W. D., 2007. A regulatory network involving Foxn4, Mash1 and delta-like 4/Notch1 generates V2a and V2b spinal interneurons from a common progenitor pool. Development. 134**,** 3427-36.

Del Bene, F., Wehman, A. M., Link, B. A., Baier, H., 2008. Regulation of neurogenesis by interkinetic nuclear migration through an apical-basal notch gradient. Cell. 134**,** 1055-65.

Dong, P. D., Provost, E., Leach, S. D., Stainier, D. Y., 2008. Graded levels of Ptf1a differentially regulate endocrine and exocrine fates in the developing pancreas. Genes Dev. 22**,** 1445-50.

Dorsky, R. I., Chang, W. S., Rapaport, D. H., Harris, W. A., 1997. Regulation of neuronal diversity in the Xenopus retina by Delta signalling. Nature. 385**,** 67-70.

Dullin, J. P., Locker, M., Robach, M., Henningfeld, K. A., Parain, K., Afelik, S., Pieler, T., Perron, M., 2007. Ptf1a triggers GABAergic neuronal cell fates in the retina. BMC Dev Biol. 7**,** 110.

Dyer, M. A., Livesey, F. J., Cepko, C. L., Oliver, G., 2003. Prox1 function controls progenitor cell proliferation and horizontal cell genesis in the mammalian retina. Nat Genet. 34**,** 53-8.

Edqvist, P. H., Hallbook, F., 2004. Newborn horizontal cells migrate bi-directionally across the neuroepithelium during retinal development. Development. 131**,** 1343-51.

Edqvist, P. H., Lek, M., Boije, H., Lindback, S. M., Hallbook, F., 2008. Axon-bearing and axon-less horizontal cell subtypes are generated consecutively during chick retinal development from progenitors that are sensitive to follistatin. BMC Dev Biol. 8**,** 46.

Edqvist, P. H., Myers, S. M., Hallbook, F., 2006. Early identification of retinal subtypes in the developing, pre-laminated chick retina using the transcription factors Prox1, Lim1, Ap2alpha, Pax6, Isl1, Isl2, Lim3 and Chx10. Eur J Histochem. 50**,** 147-54.

Fantl, V., Stamp, G., Andrews, A., Rosewell, I., Dickson, C., 1995. Mice lacking cyclin D1 are small and show defects in eye and mammary gland development. Genes Dev. 9**,** 2364-72.

Fischer, A. J., Stanke, J. J., Aloisio, G., Hoy, H., Stell, W. K., 2007. Heterogeneity of horizontal cells in the chicken retina. J Comp Neurol. 500**,** 1154-71.

Fujitani, Y., Fujitani, S., Luo, H., Qiu, F., Burlison, J., Long, Q., Kawaguchi, Y., Edlund, H., Macdonald, R. J., Furukawa, T., Fujikado, T., Magnuson, M. A., Xiang, M., Wright, C. V., 2006. Ptf1a determines horizontal and amacrine cell fates during mouse retinal development. Development. 133**,** 4439-50.

Gallego, A., 1986. Chapter 7. Comparative studies on horizontal cells and a note on microglial cells. Prog. Retin. Res. 5. 165-206.

Genis-Galvez, J. M., Prada, F., Armengol, J.A, 1979. Evidence of three horizontal cells in the chick retina. Jpn.J.Ophtamol. 23**,** 378-387.

Glasgow, S. M., Henke, R. M., Macdonald, R. J., Wright, C. V., Johnson, J. E., 2005. Ptf1a determines GABAergic over glutamatergic neuronal cell fate in the spinal cord dorsal horn. Development. 132**,** 5461-9.

Godbout, R., Andison, R., 1996. Elevated levels of cyclin D1 mRNA in the undifferentiated chick retina. Gene. 182**,** 111-5.

Hayes, S., Nelson, B. R., Buckingham, B., Reh, T. A., 2007. Notch signaling regulates regeneration in the avian retina. Dev Biol. 312**,** 300-11.

Henke, R. M., Savage, T. K., Meredith, D. M., Glasgow, S. M., Hori, K., Dumas, J., MacDonald, R. J., Johnson, J. E., 2009. Neurog2 is a direct downstream target of the Ptf1a-Rbpj transcription complex in dorsal spinal cord. Development. 136**,** 2945-54.

Henrique, D., Hirsinger, E., Adam, J., Le Roux, I., Pourquie, O., Ish-Horowicz, D., Lewis, J., 1997. Maintenance of neuroepithelial progenitor cells by Delta-Notch signalling in the embryonic chick retina. Curr Biol. 7**,** 661-70.

Hinds, J. W., Hinds, P. L., 1979. Differentiation of photoreceptors and horizontal cells in the embryonic mouse retina: an electron microscopic, serial section analysis. J Comp Neurol. 187**,** 495-511.

Hori, K., Cholewa-Waclaw, J., Nakada, Y., Glasgow, S. M., Masui, T., Henke, R. M., Wildner, H., Martarelli, B., Beres, T. M., Epstein, J. A., Magnuson, M. A., Macdonald, R. J., Birchmeier, C., Johnson, J. E., 2008. A nonclassical bHLH Rbpj transcription factor complex is required for specification of GABAergic neurons independent of Notch signaling. Genes Dev. 22**,** 166-78.

Hoshino, M., Nakamura, S., Mori, K., Kawauchi, T., Terao, M., Nishimura, Y. V., Fukuda, A., Fuse, T., Matsuo, N., Sone, M., Watanabe, M., Bito, H., Terashima, T., Wright, C. V., Kawaguchi, Y., Nakao, K., Nabeshima, Y., 2005. Ptf1a, a bHLH transcriptional gene, defines GABAergic neuronal fates in cerebellum. Neuron. 47**,** 201-13.

Hughes, S. H., Greenhouse, J. J., Petropoulos, C. J., Sutrave, P., 1987. Adaptor plasmids simplify the insertion of foreign DNA into helper-independent retroviral vectors. J Virol. 61**,** 3004-12.

Inoue, T., Hojo, M., Bessho, Y., Tano, Y., Lee, J. E., Kageyama, R., 2002. Math3 and NeuroD regulate amacrine cell fate specification in the retina. Development. 129**,** 831-42.

Jadhav, A. P., Mason, H. A., Cepko, C. L., 2006. Notch 1 inhibits photoreceptor production in the developing mammalian retina. Development. 133**,** 913-23.
Jusuf, P. R., Almeida, A. D., Randlett, O., Joubin, K., Poggi, L., Harris, W. A., 2011. Origin and determination of inhibitory cell lineages in the vertebrate retina. J Neurosci. 31**,** 2549-62.
Jusuf, P. R., Harris, W. A., 2009. Ptf1a is expressed transiently in all types of amacrine cells in the embryonic zebrafish retina. Neural Dev. 4**,** 34.
Kawaguchi, Y., Cooper, B., Gannon, M., Ray, M., MacDonald, R. J., Wright, C. V., 2002. The role of the transcriptional regulator Ptf1a in converting intestinal to pancreatic progenitors. Nat Genet. 32**,** 128-34.
Krapp, A., Knofler, M., Ledermann, B., Burki, K., Berney, C., Zoerkler, N., Hagenbuchle, O., Wellauer, P. K., 1998. The bHLH protein PTF1-p48 is essential for the formation of the exocrine and the correct spatial organization of the endocrine pancreas. Genes Dev. 12**,** 3752-63.
Lemercier, C., To, R. Q., Carrasco, R. A., Konieczny, S. F., 1998. The basic helix-loop-helix transcription factor Mist1 functions as a transcriptional repressor of myoD. EMBO J. 17**,** 1412-22.
Li, S., Mo, Z., Yang, X., Price, S. M., Shen, M. M., Xiang, M., 2004. Foxn4 controls the genesis of amacrine and horizontal cells by retinal progenitors. Neuron. 43**,** 795-807.
Liu, W., Mo, Z., Xiang, M., 2001. The Ath5 proneural genes function upstream of Brn3 POU domain transcription factor genes to promote retinal ganglion cell development. Proc Natl Acad Sci U S A. 98**,** 1649-54.
Livesey, F. J., Cepko, C. L., 2001. Vertebrate neural cell-fate determination: lessons from the retina. Nat Rev Neurosci. 2**,** 109-18.
Mao, W., Yan, R. T., Wang, S. Z., 2009. Proneural gene ash1 promotes amacrine cell production in the chick retina. Dev Neurobiol. 69**,** 88-104.
Marquardt, T., Gruss, P., 2002. Generating neuronal diversity in the retina: one for nearly all. Trends Neurosci. 25**,** 32-8.
Masui, T., Long, Q., Beres, T. M., Magnuson, M. A., MacDonald, R. J., 2007. Early pancreatic development requires the vertebrate Suppressor of Hairless (RBPJ) in the PTF1 bHLH complex. Genes Dev. 21**,** 2629-43.
Masui, T., Swift, G. H., Deering, T., Shen, C., Coats, W. S., Long, Q., Elsasser, H. P., Magnuson, M. A., MacDonald, R. J., 2010. Replacement of Rbpj with Rbpjl in the PTF1 complex controls the final maturation of pancreatic acinar cells. Gastroenterology. 139**,** 270-80.
Masui, T., Swift, G. H., Hale, M. A., Meredith, D. M., Johnson, J. E., Macdonald, R. J., 2008. Transcriptional autoregulation controls pancreatic Ptf1a expression during development and adulthood. Mol Cell Biol. 28**,** 5458-68.
Matter-Sadzinski, L., Matter, J. M., Ong, M. T., Hernandez, J., Ballivet, M., 2001. Specification of neurotransmitter receptor identity in developing retina: the chick ATH5 promoter integrates the positive and negative effects of several bHLH proteins. Development. 128**,** 217-31.
Matter-Sadzinski, L., Puzianowska-Kuznicka, M., Hernandez, J., Ballivet, M., Matter, J. M., 2005. A bHLH transcriptional network regulating the specification of retinal ganglion cells. Development. 132**,** 3907-21.
Meredith, D. M., Masui, T., Swift, G. H., MacDonald, R. J., Johnson, J. E., 2009. Multiple transcriptional mechanisms control Ptf1a levels during neural development including autoregulation by the PTF1-J complex. J Neurosci. 29**,** 11139-48.

Rodolosse, A., Campos, M. L., Rooman, I., Lichtenstein, M., Real, F. X., 2009. p/CAF modulates the activity of the transcription factor p48/Ptf1a involved in pancreatic acinar differentiation. Biochem J. 418**,** 463-73.

Roger, J., Brajeul, V., Thomasseau, S., Hienola, A., Sahel, J. A., Guillonneau, X., Goureau, O., 2006. Involvement of Pleiotrophin in CNTF-mediated differentiation of the late retinal progenitor cells. Dev Biol. 298**,** 527-39.

Sellick, G. S., Barker, K. T., Stolte-Dijkstra, I., Fleischmann, C., Coleman, R. J., Garrett, C., Gloyn, A. L., Edghill, E. L., Hattersley, A. T., Wellauer, P. K., Goodwin, G., Houlston, R. S., 2004. Mutations in PTF1A cause pancreatic and cerebellar agenesis. Nat Genet. 36**,** 1301-5.

Sicinski, P., Donaher, J. L., Parker, S. B., Li, T., Fazeli, A., Gardner, H., Haslam, S. Z., Bronson, R. T., Elledge, S. J., Weinberg, R. A., 1995. Cyclin D1 provides a link between development and oncogenesis in the retina and breast. Cell. 82**,** 621-30.

Silva, A. O., Ercole, C. E., McLoon, S. C., 2003. Regulation of ganglion cell production by Notch signaling during retinal development. J Neurobiol. 54**,** 511-24.

Skowronska-Krawczyk, D., Chiodini, F., Ebeling, M., Alliod, C., Kundzewicz, A., Castro, D., Ballivet, M., Guillemot, F., Matter-Sadzinski, L., Matter, J. M., 2009. Conserved regulatory sequences in Atoh7 mediate non-conserved regulatory responses in retina ontogenesis. Development. 136**,** 3767-77.

Skowronska-Krawczyk, D., Matter-Sadzinski, L., Ballivet, M., Matter, J. M., 2005. The basic domain of ATH5 mediates neuron-specific promoter activity during retina development. Mol Cell Biol. 25**,** 10029-39.

Suga, A., Taira, M., Nakagawa, S., 2009. LIM family transcription factors regulate the subtype-specific morphogenesis of retinal horizontal cells at post-migratory stages. Dev Biol. 330**,** 318-28.

Tanabe, K., Takahashi, Y., Sato, Y., Kawakami, K., Takeichi, M., Nakagawa, S., 2006. Cadherin is required for dendritic morphogenesis and synaptic terminal organization of retinal horizontal cells. Development. 133**,** 4085-96.

Wang, S. W., Kim, B. S., Ding, K., Wang, H., Sun, D., Johnson, R. L., Klein, W. H., Gan, L., 2001. Requirement for math5 in the development of retinal ganglion cells. Genes Dev. 15**,** 24-9.

Wildner, H., Muller, T., Cho, S. H., Brohl, D., Cepko, C. L., Guillemot, F., Birchmeier, C., 2006. dILA neurons in the dorsal spinal cord are the product of terminal and non-terminal asymmetric progenitor cell divisions, and require Mash1 for their development. Development. 133**,** 2105-13.

Yamada, M., Terao, M., Terashima, T., Fujiyama, T., Kawaguchi, Y., Nabeshima, Y., Hoshino, M., 2007. Origin of climbing fiber neurons and their developmental dependence on Ptf1a. J Neurosci. 27**,** 10924-34.

Yang, X. J., 2002. Retrovirus-mediated gene expression during chick visual system development. Methods. 28**,** 396-401.

Yaron, O., Farhy, C., Marquardt, T., Applebury, M., Ashery-Padan, R., 2006. Notch1 functions to suppress cone-photoreceptor fate specification in the developing mouse retina. Development. 133**,** 1367-78.

Young, R. W., 1985. Cell differentiation in the retina of the mouse. Anat Rec. 212**,** 199-205.

Zecchin, E., Mavropoulos, A., Devos, N., Filippi, A., Tiso, N., Meyer, D., Peers, B., Bortolussi, M., Argenton, F., 2004. Evolutionary conserved role of ptf1a in the specification of exocrine pancreatic fates. Dev Biol. 268**,** 174-84.

Zheng, M. H., Shi, M., Pei, Z., Gao, F., Han, H., Ding, Y. Q., 2009. The transcription factor RBP-J is essential for retinal cell differentiation and lamination. Mol Brain. 2**,** 38.

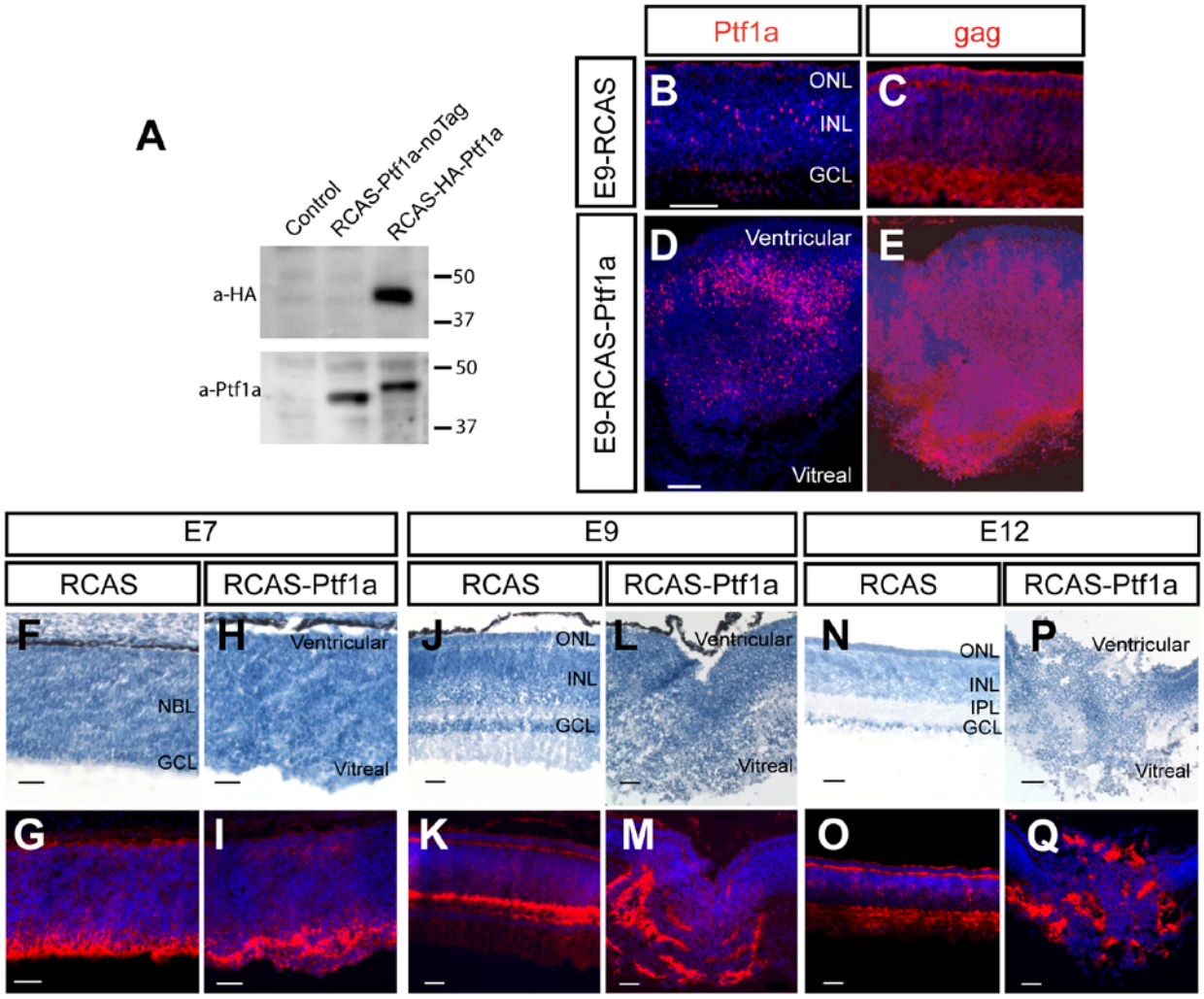

Fig. 1: Mis/overexpression of Ptf1a affects retinal structure.
(A) Lysates from DF1 cells transfected with the RCAS-Ptf1a plasmids or not (Control) were harvested, and the expression of exogenous Ptf1a proteins was monitored by western blotting using anti-Ptf1a and anti-HA antibodies. RCAS-Ptf1a-noTag: RCAS-Ptf1a without HA-Tag, RCAS-HA-Ptf1a: RCAS-Ptf1a with HA-tag. (B-E) The RCAS-infected (B-C) and RCASPtf1a-infected (D-E) retinal sections were stained with anti-Ptf1a (B,D) or anti-gag (p27) (C,E) antibodies at E9. (F-Q) The RCAS-infected (F-G,J -K,N-O) and RCAS-Ptf1a-infected (H-I,L-M,P-Q) retinal sections were co-stained with hemalun (F,H,J,L,N,P) and anti-gag (3c2) antibodies (G,I,K,M,O,Q). In B-E,G,I,K,M,O,Q, retinal sections were counterstained with DAPI. ONL, outer nuclear layer; INL, inner nuclear layer; IPL, inner plexiform layer; GCL, ganglion cell layer; NBL, neuroblastic layer. Bars: 50 µm (B-E in B and D), 25 µm (F-Q).

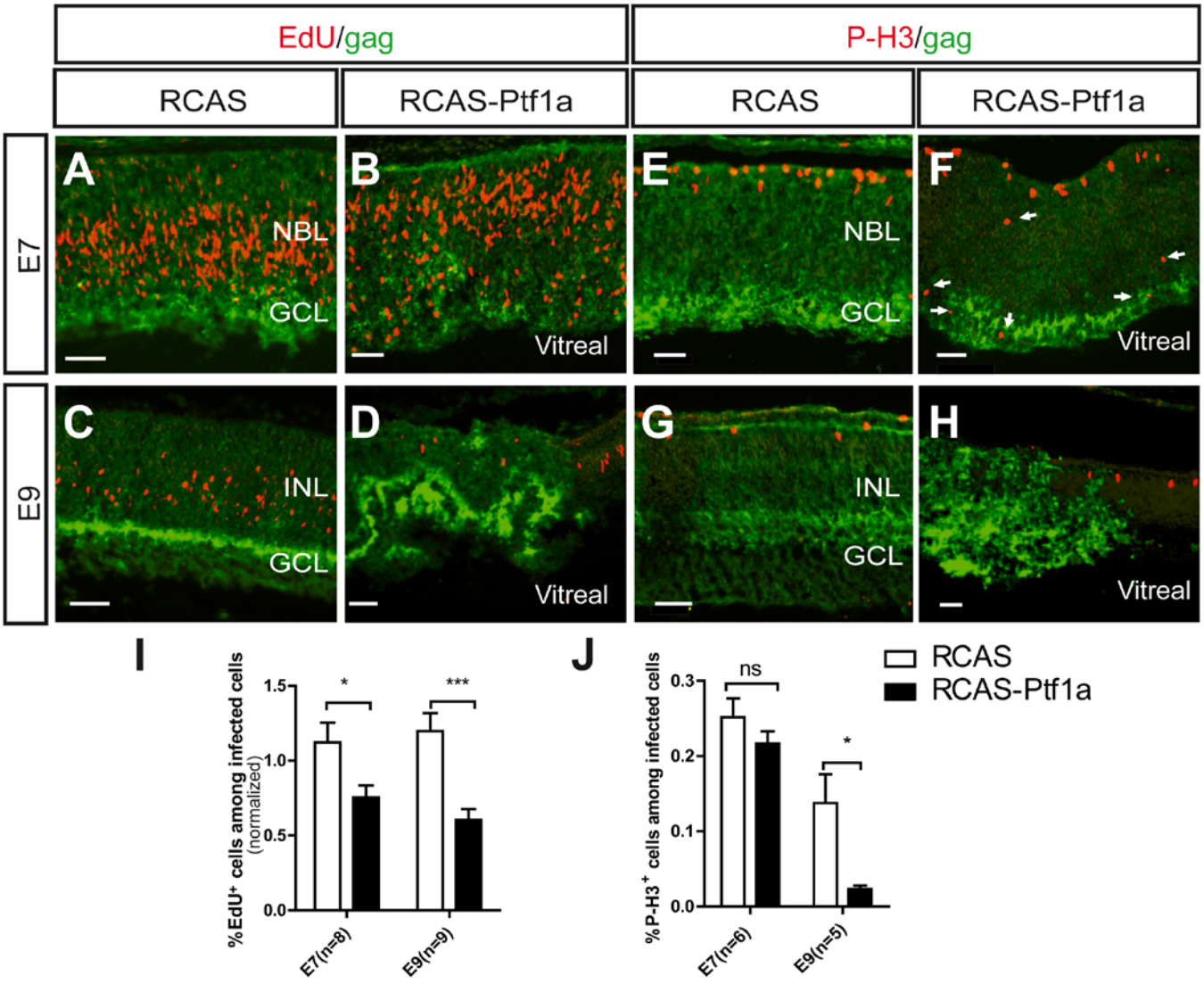

Fig. 2: Effects of Ptf1a mis/overexpression on retinal progenitor cell proliferation. (A-H) Sections from the RCAS-infected (A,C,E,G) and the RCAS-Ptf1a-infected (B,D,F,H) retinas were stained with EdU and anti-gag (3c2) antibodies (A-D) or with anti-P-H3 and antigag antibodies (E-H) at E7 and E9. In F, arrows point to P-H3 positive cells in an ectopic location in the RCAS-Ptf1a-infected retinas. (I-J) Quantitative analysis of EdU-positive (I) or P-H3-positive cells (J) among the RCAS- and RCAS-Ptf1a-infected cells at E7 and E9. Values represent the mean ± s.e.m. The percentage of EdU-positive cells among the infected cells was normalized by the percentage of EdU-positive cells among the non-infected cells for each embryo. NBL, neuroblastic layer; GCL, ganglion cell layer; INL, inner nuclear layer. Bars: 25 μm.

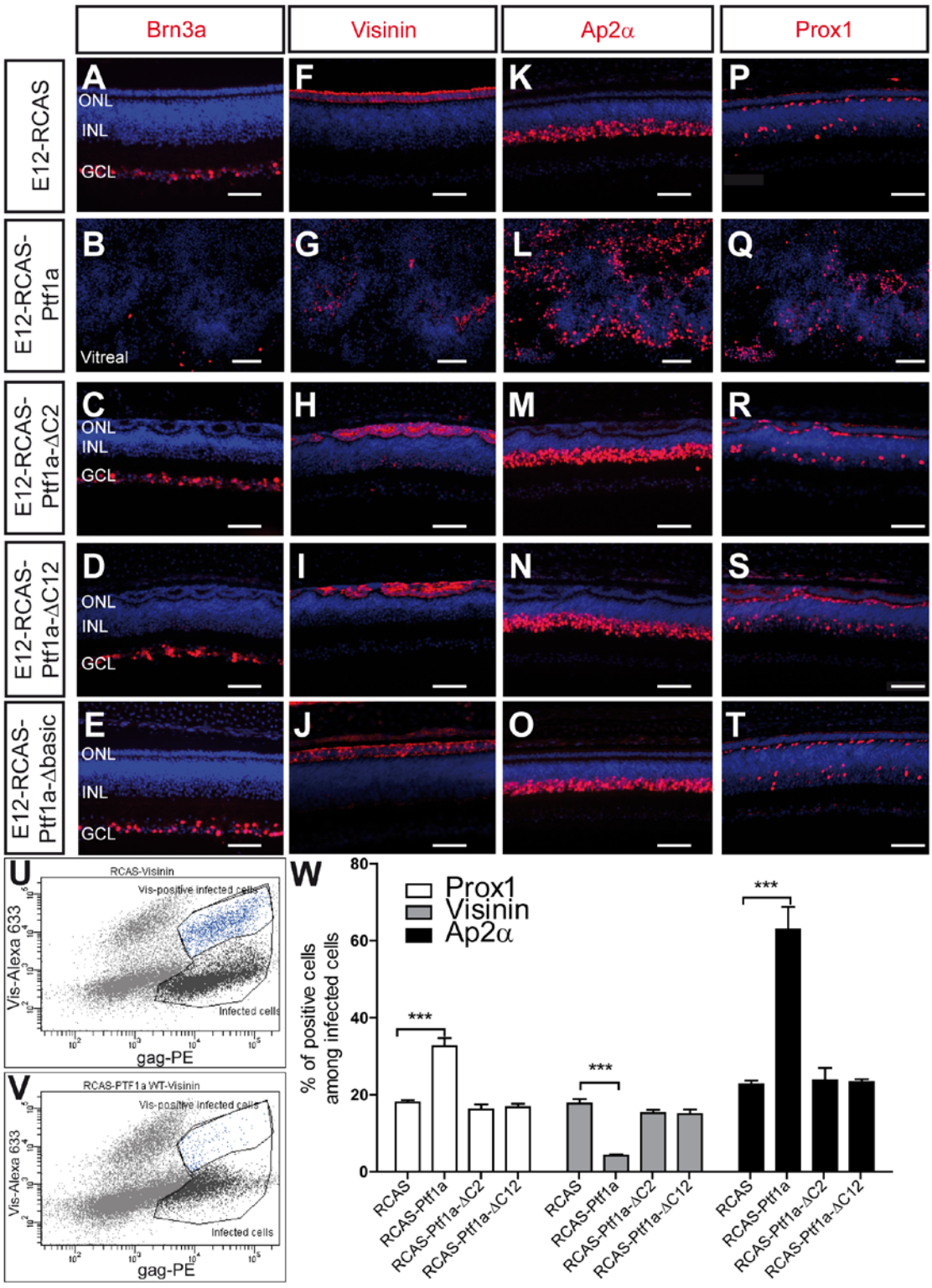

Fig. 3: Effects of wild-type and mutant forms of Ptf1a on retinal cell differentiation. (A-T) The RCAS-infected (A,F,K,P), RCAS-Ptf1a-infected (B,G,L,Q), RCAS-Ptf1a-ΔC2-infected (C,H,M,R), RCAS-Ptf1a-ΔC12-infected (D,I,N,S) and RCAS-Ptf1a-Δbasic-infected (E,J,O,T) patches from E12 retinas were immunostained using anti-Brn3a (A-E), anti-Visinin (F-J), anti-Ap2α (K-O), and anti-Prox1 (P-T) antibodies. For clarity, the gag labeling is not represented. Retinal sections were counterstained with DAPI. (U-V) Representative flow cytometry analysis after staining the RCAS-infected (U) and RCAS-Ptf1a-infected (V) dissociated cells with anti-gag (p27) and anti-Visinin antibodies at E12. (W) Quantitative analysis of Visinin-, Ap2α- and Prox1-positive cells among the infected cells at E12. Values represent the mean ± s.e.m of at least four separate eye counts. ONL, outer nuclear layer; INL, inner nuclear layer; GCL, ganglion cell layer; PE, Phycoerythrin; Alexa633, AlexaFluor633. Bars: 50 µm

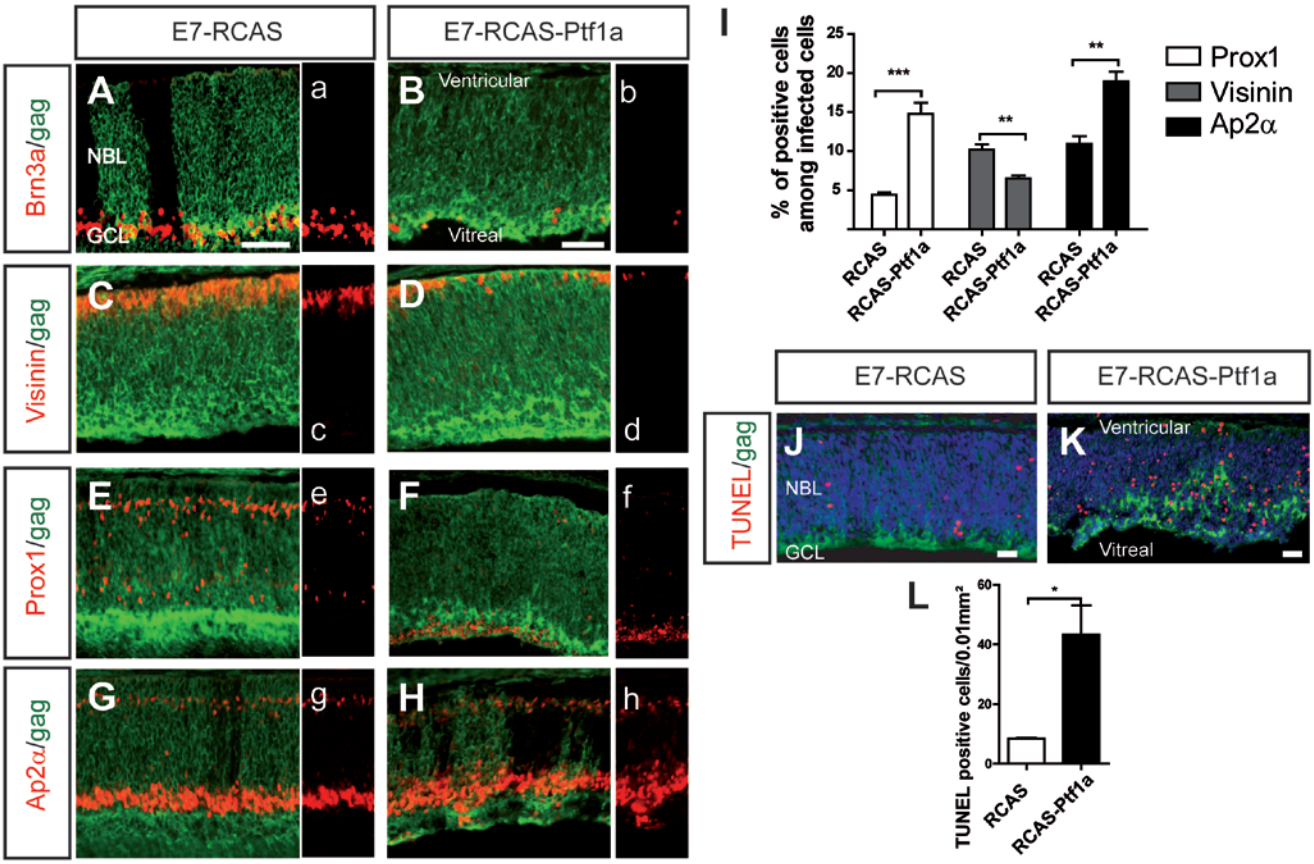

Fig. 4: Retinal cell type representation is modified in E7 retinas prior to lamination defects.
(A-H) The E7 RCAS-infected (A,C,E,G) and RCAS-Ptf1a-infected (B,D,F,H) retinal patches were immunostained using an anti-gag antibody and either anti-Brn3a (A-B), anti-Visinin (CD), anti-Prox1 (E-F) or anti-Ap2α (G-H) antibodies. Cell type-specific labeling in panels A-H was represented without gag labeling in panels a-h, respectively. (I) Quantitative analysis of Visinin-, Ap2α- or Prox1-positive cells among the infected cells. The values represent the mean ± s.e.m of at least four separate retinal counts and are representative of two independent injections. (J-L) Cells undergoing apoptosis were TUNEL-labeled at E7 in the RCASinfected (J) and RCAS-Ptf1a-infected (K) patches detected using anti-gag (p27) antibody. Sections in J and K were counterstained with DAPI. (L) Quantitative analysis of the number of apoptotic cells per area in the RCAS- and RCAS-Ptf1a-infected patches at E7. The values represent the mean ± s.e.m of at least three separate retinas. NBL, neuroblastic layer; GCL, ganglion cell layer. Bars: 50 µm (A,C,E, and G in A and B,D,F, and H in B), 25 µm (J,K).

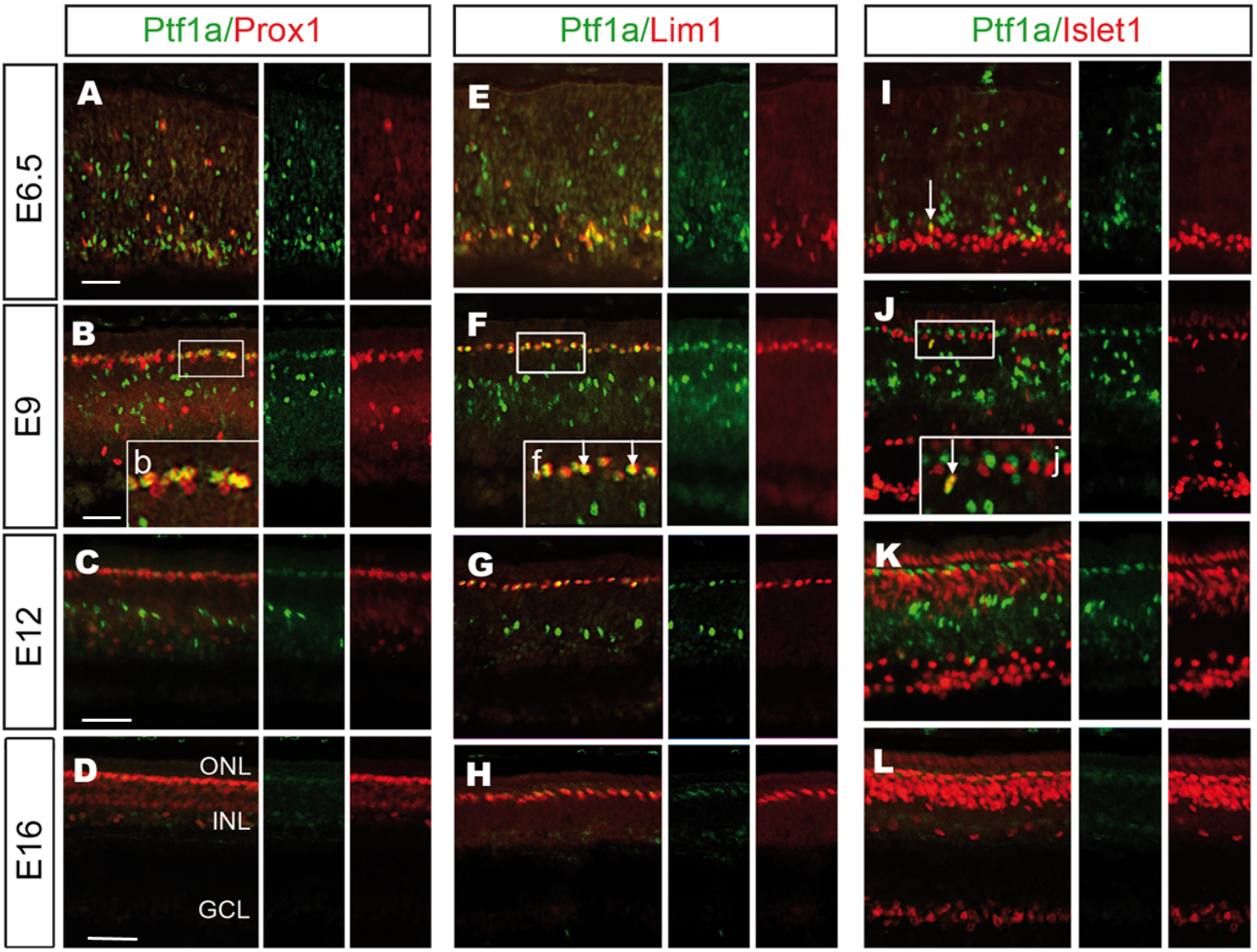

Fig. 5: Ptf1a expression in subtypes of developing horizontal cells. Epifluorescence micrographs show Ptf1a, Prox1 (A-D), Ptf1a, Lim1 (E-H), and Ptf1a, Islet1 (I-L) double-labeling of E6.5, E9, E12 and E16 chick retinas, and the corresponding split fluorescence images are to the right of each panel. Insets in b, f, and j are higher magnifications of the boxes in B, F and J. Arrows point at double-labeled cells. GCL, ganglion cell layer; INL, inner nuclear layer; ONL, outer nuclear layer. Bars: 25 µm.

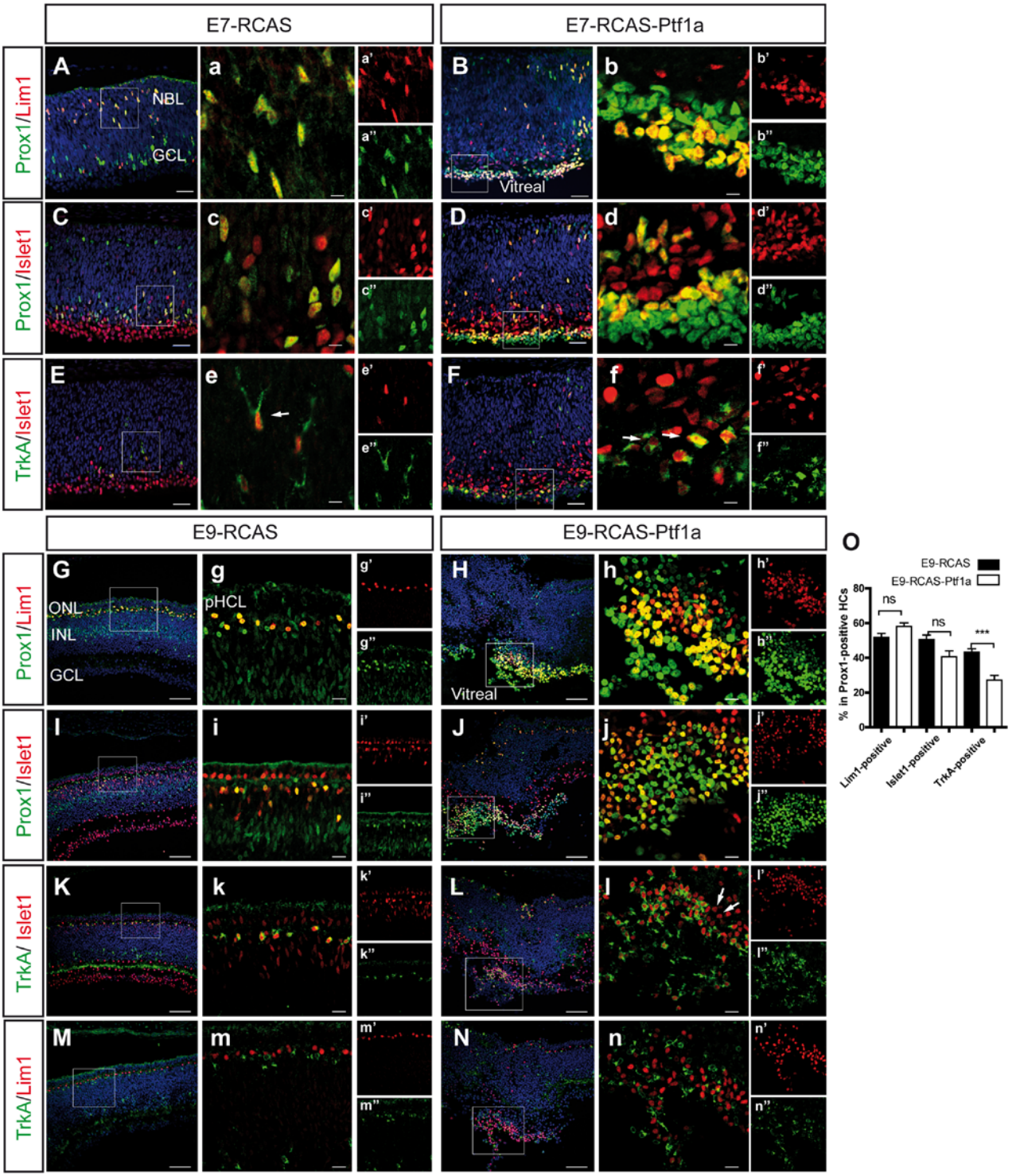

Fig. 6: Ptf1a mis/overexpression is sufficient to increase the number of all horizontal cell subtypes.

(A-F) The RCAS-infected (A,C,E) and RCAS-Ptf1a-infected (B,D,F) patches were double immunostained at E7 with either anti-Lim1 and anti-Prox1 antibodies for H1 cells (A-B), anti-Islet1 and anti-Prox1 antibodies for H2 and H3 cells (C-D) or anti-Islet1 and anti-TrkA antibodies for H3 cells (E-F). a-f are higher magnifications of the boxes in A-F, respectively. a′-f′ and a″-f″ are split fluorescence images of a-f. Arrows point to some double-positive cells. (G-N) The RCAS-infected (G,I,K,M) and RCAS-Ptf1a-infected (H,J,L,N) patches at E9 were double immunostained with either anti-Lim1 and anti-Prox1 (G-H), anti-Islet1 and anti-Prox1 (I-J), anti-Islet1 and anti-TrkA (K-L) or anti-TrkA and anti-Lim1 antibodies (M-N). g-n are higher magnifications of boxes in G-N, respectively. g′-n′ and g″-n″ are split fluorescent images of g-n, respectively. Arrows point to some Islet1-positive/TrkA-negative cells. (O) The quantification of Lim1- (H1), Islet1- (H2-H3) and TrkA-positive (H3) cells among the Prox1-positive HCs in the RCAS- and RCAS-Ptf1a-infected patches at E9. The values represent the mean ± s.e.m. NBL, neuroblastic layer; ONL, outer nuclear layer; INL, inner nuclear layer; GCL, ganglion cell layer; pHCL, prospective horizontal cell layer. Bars: 25 μm (A-F), 5 μm (a-f), 50 μm (G-N), 10 μm (g-n).

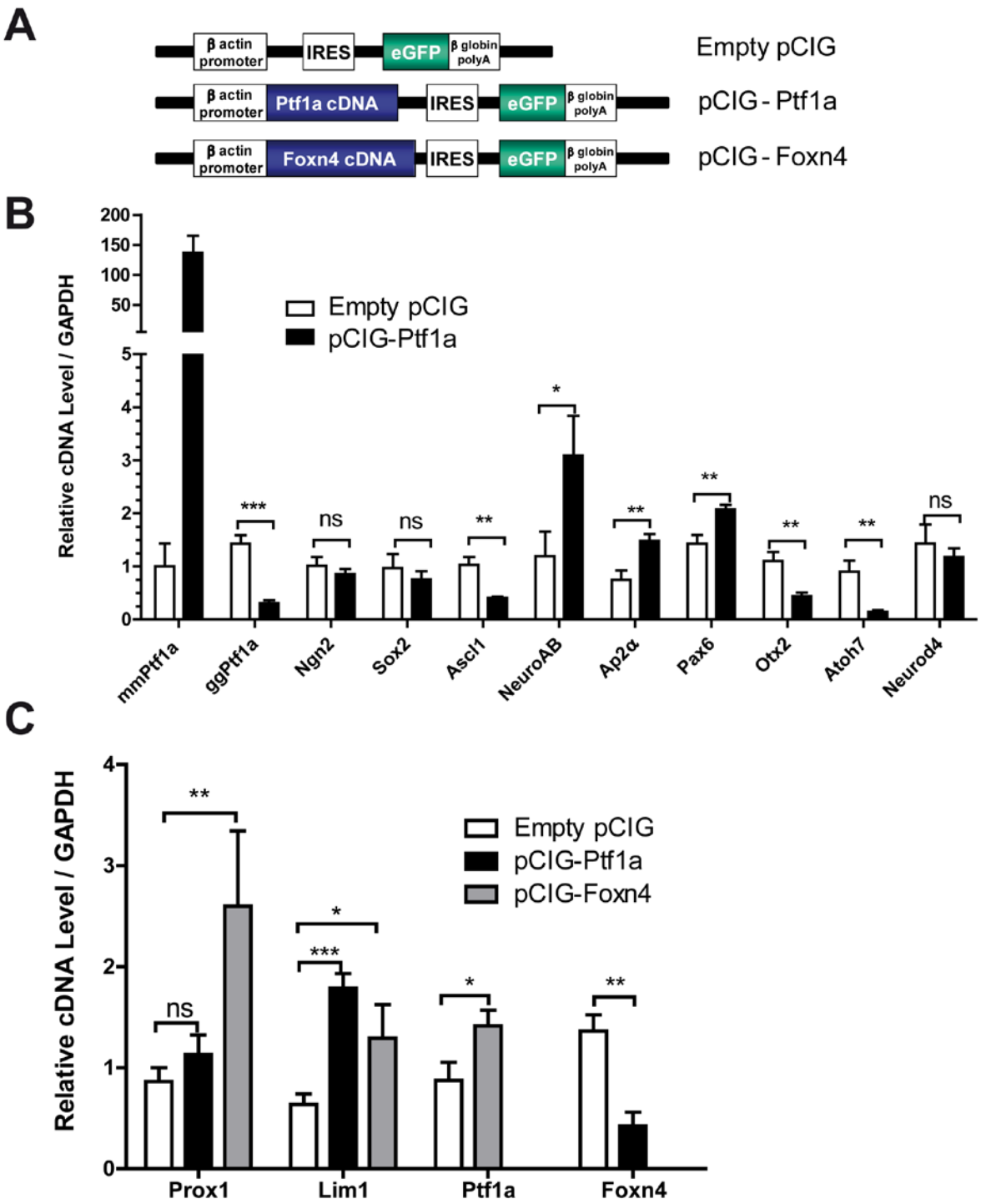

Fig. 7: Changes in retinogenic factor mRNA expression following Ptf1a overexpression. (A) Schematic structure of pCIG expression vectors. IRES, internal ribosomal entry site. (B) The expression level of candidate genes was analyzed by quantitative PCR (qPCR) on mRNA from GFP-positive sorted retinal cells electroporated at E5 with either pCIG-GFP (Empty pCIG) or pCIG-Ptf1a-GFP (pCIG-Ptf1a). mmPtf1a, mouse Ptf1a; ggPtf1a, chick Ptf1a. (C) The expression level of a subset of genes involved in HC development was assessed by qPCR on mRNA isolated from GFP-positive sorted retinal cells electroporated at E5 with empty pCIG, pCIG-Ptf1a or pCIG-Foxn4-GFP (pCIG-Foxn4). Data represent the mean ± s.e.m of a least four retinas.

Table S1: Summary list of primers used in this study.

Name	Primer Sequence 5'->3'	Reference
Actin Forward	CATCACCATTGGCAATGAGAG	
Actin Reverse	TGGACAGGGAGGCCAGGATAG	
Ap2α Forward	AGAGTTCACCGACCTGCT	
Ap2α Reverse	GCCGTGCGAGATGAGGTTGA	
ggPtf1a Forward	GAAGGCGAACGCCAAACCCT	
ggPtf1a Reverse	GTTGATTGCCCTTAGAGTCC	
mmPtf1a Forward	GAAGGTCATCATCTGCCATCG	
mmPtf1a Reverse	TCAGGACACAAACTCAAARGGTG	
Ascl1 Forward	AGGGAACCACGTTTATGCAG	(Hayes et al., 2007)
Ascl1 Reverse	TTATACAGGGCCTGGTGAGC	(Hayes et al., 2007)
Atoh7 Forward	CTGTGAACACTTTCATCCAGAG	
Atoh7 Reverse	CTAATTAGCTATTTGAAAGTGTTCAG	
Foxn4 Forward	GCTGCCATTCATAGGAGCAT	(Hayes et al., 2007)
Foxn4 Reverse	CTGGGTCTGGATCTGGTGAT	(Hayes et al., 2007)
GAPDH Forward	TGCCCAGAACATCATCCCAGCG	
GAPDH Reverse	TGGGGGTTGGCACACGGAAA	
Lim1 Forward	TTCTCCTCGATATCCGTCAACG	
Lim1 Reverse	CACCGTAACAACAAGCAGACTAG	
NeuroAB/bHLHb4 Forward	ACCCTCAACCCCTTCGGACA	
NeuroAB/bHLHb4 Reverse	AGTGTTTGCAGAGCGCGGAG	
Ngn2 Forward	GCTGTCTCCGTGATTTACGAG	
Ngn2 Reverse	CCCTTCCCTTCCCTCTACAGTT	
Otx2 Reverse	TTAACTTCCAGGAGGCGGTTTGG	
Otx2 Forward	ATGGGTGCCAATGCGGTCACCA	
Pax6 Forward	TCCAGTTCAAGTTCCTGGCAG	
Pax6 Reverse	GTGTTACAGCGTAGGGCACAG	
Prox1 Forward	CAGGGCCCTGAACATGCACTA	
Prox1 Reverse	CTCTTGTAGGCAGTTGGGGGA	
Rbpjl Forward (TC_237853)	CCCTCGCAGAAGAAGCAGTC	
Rbpjl Reverse	TGTGAGCGCAGGCGGTTGAA	
Sox2 Forward	AGGCTATGGGATGATGCAAG	(Hayes et al., 2007)
Sox2 Reverse	GTAGGTAGGCGATCCGTTCA	(Hayes et al., 2007)
Neurod4/Ath3 Forward	AACCCCCCCGACTGCACCACT	.
Neurod4/Ath3 Reverse	CTGACCGAAGGGTAGTGAGCCA	.

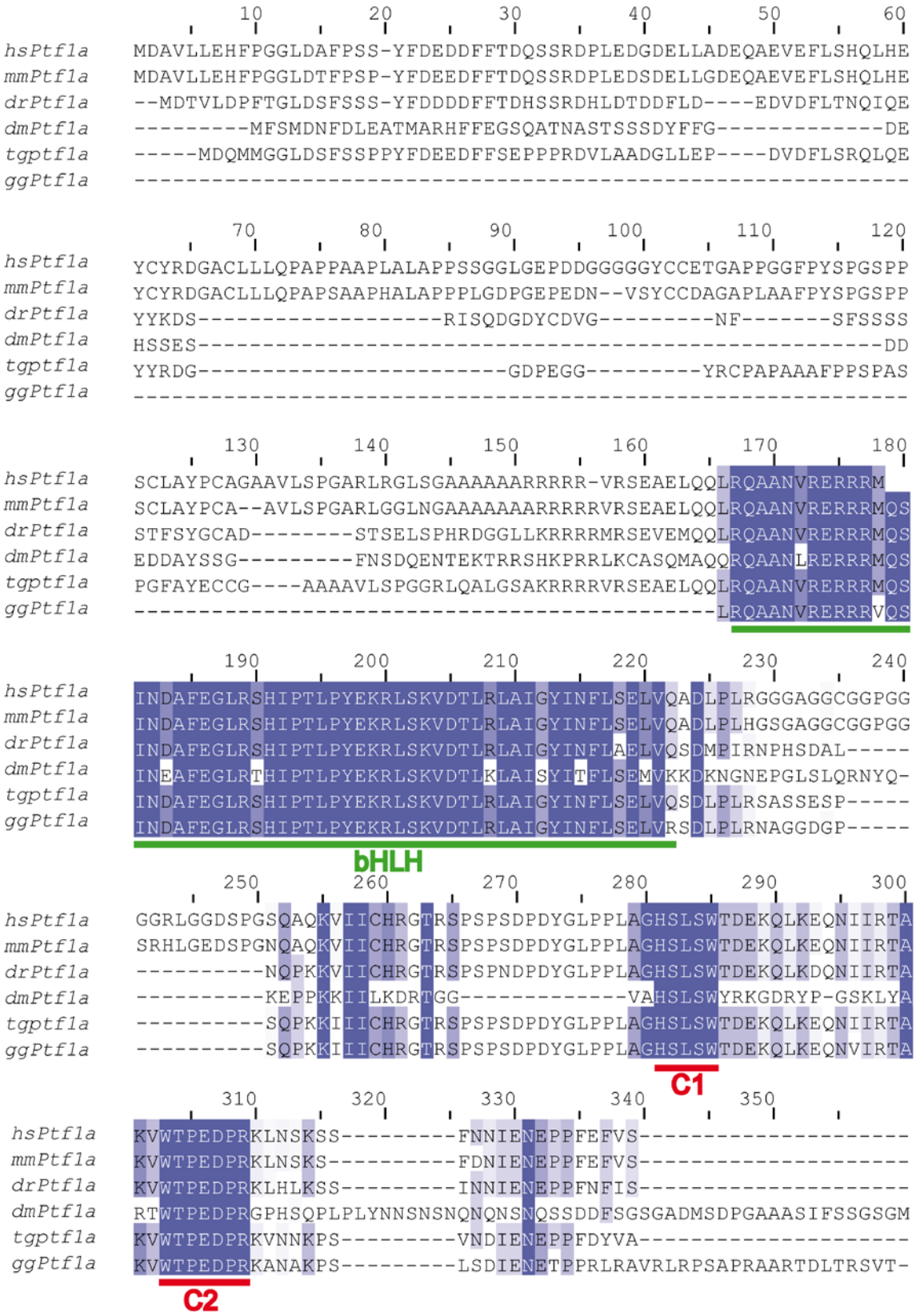

Fig. S1: The partial chick Ptf1a protein sequence.

Alignment of the sequences of the human (hs), mouse (mm), zebrafish (dr), *drosophilia* (dm) (Fer1), bird zebra finch (tg, *Taeniopygia guttata,* accession number XM_002190193) and partial chick (gg) Ptf1a proteins. The C1 and C2 domains (deep-blue shading, red underlining) are identified within the C-terminal part of chick Ptf1a protein. The green underline highlights the conserved bHLH domain (deep-blue staining). The sequences were aligned using Vector NTI Software (Invitrogen).

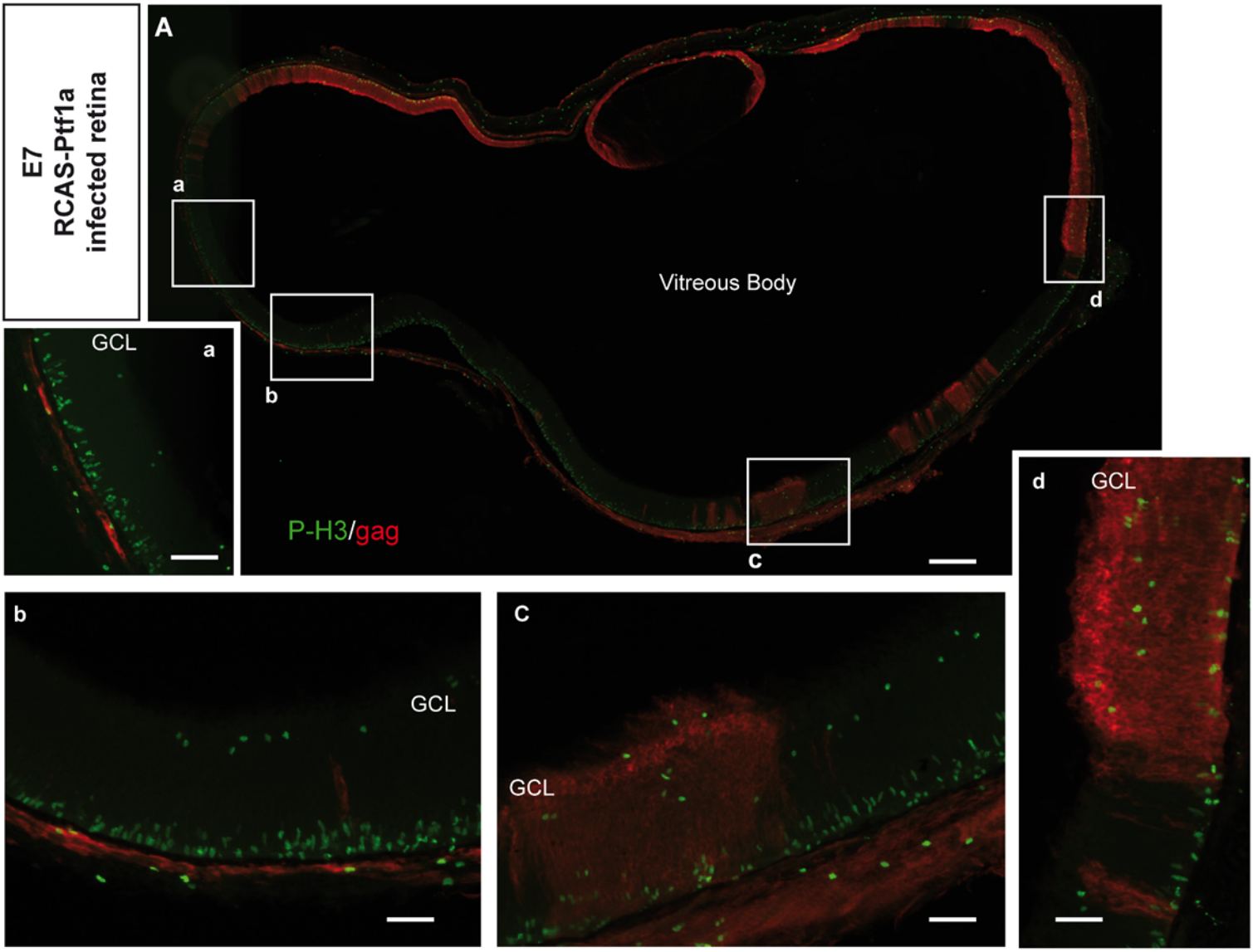

Fig. S2: Location of P-H3 positive cells in RCAS-Ptf1a-infected retina at E7.

(A) A retina infected with RCAS-Ptf1a was immunostained at E7 with anti-gag (3c2) and anti-P-H3 antibodies. (a-d) are higher magnifications of boxes in A. GCL, ganglion cell layer. Bars: 250 µm (A), 50 µm (a-d).

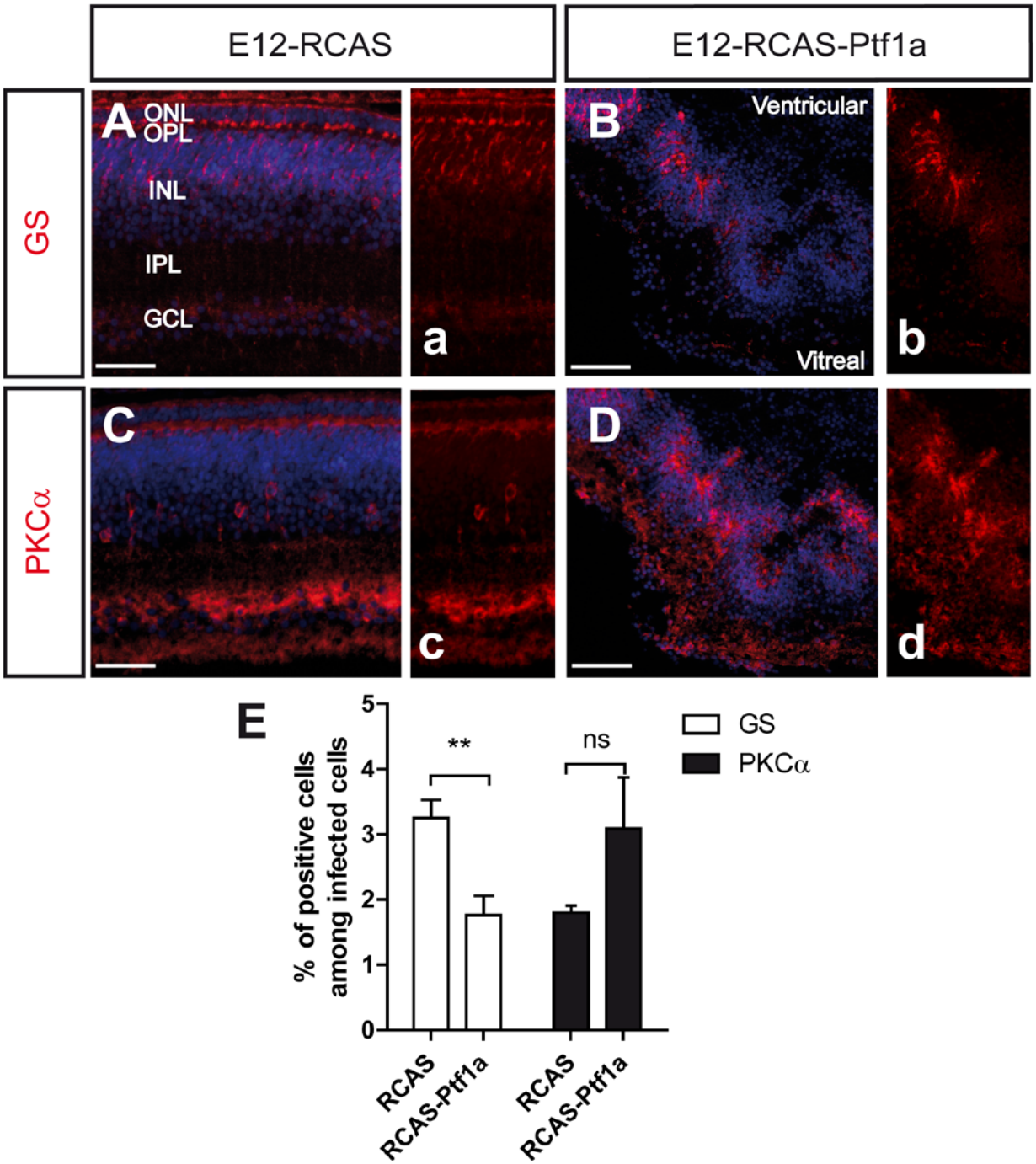

Fig. S3: Effects of Ptf1a misexpression on late born retinal cells.

(A-D) The RCAS-infected (A,C) and RCAS-Ptf1a-infected (B,D) patches from E12 retinas were immunostained using anti-Glutamine Synthetase (GS) (A-B) and anti-Protein Kinase Cα (PKCα) (C-D) antibodies. For clarity, gag labeling is not represented. The cell type-specific labeling in images A-D was represented without DAPI staining in images a-d, respectively. **(E)** The number of GS-positive and PKCα-positive cells among the infected cells was scored using manual counting on dissociated retinal cells immunostained with anti-PKCα or anti-GS and anti-gag antibodies. The data represent the mean ± s.e.m of at least four separate retina counts. ONL, outer nuclear layer; OPL, outer plexiform layer; INL, inner nuclear layer; IPL, inner plexiform layer; GCL, ganglion cell layer. Bars: 25 µm (A,C), 50 µm (B,D).

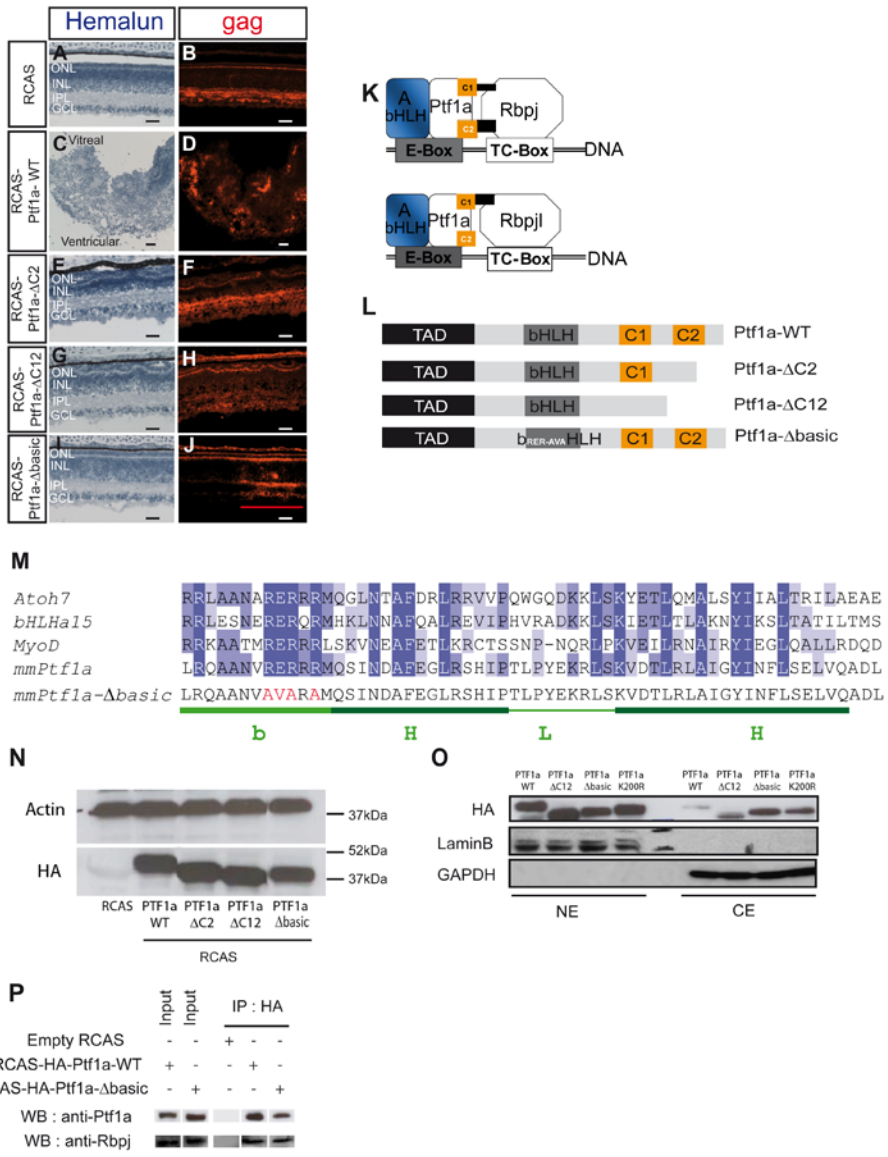

Fig. S4: Generation of Ptf1a mutant forms and their effects on chick retinal lamination.

(A-J) The E12 retinas infected with the indicated RCAS virus were immunostained using anti-gag (3c2) antibody to detect infected patches (B,D,F,H,J) and hemalun-stained (A,C,E,G,I) to label nuclei. The red line in J indicates the infected area. (**K**) Schematic diagrams of PTF1 complex formed by Ptf1a/p48, an E-protein (AbHLH) and either Rbpj or Rbpjl. Ptf1a interacts with Rbpj with its C2 and C1 domains, whereas only the C1 domain is required for its interaction with Rbpjl (Beres et al., 2006). (**L**) The schematic structure of the Ptf1a mutant forms generated in this study. The Ptf1a protein contains a transactivation domain within its N-terminal (Rodolosse et al., 2009) and a bHLH DNA-binding domain necessary for its heterodimerization with other AbHLH factors. The C1 and C2 Rbp-interacting domains are located within the C-terminal part of Ptf1a. **(M)** The alignment of the bHLH domain sequences of Atoh7, bHLHa15 (Mist1), MyoD and mouse Ptf1a (mmPtf1a) highlight the strong conservation of RER-R amino acids within the basic domain. In the Ptf1a-Δbasic mutant form, these RER-R amino acids were replaced by AVA-A. **(N)** Whole cell lysates from DF1 cells were harvested, and the expression level of HA-tagged Ptf1a proteins was assessed by western blotting with anti-HA antibodies. (**O)** The lysates from DF1 were fractionated to isolate nuclear (NE) from cytosolic extracts (CE). The level of HA-tagged Ptf1a proteins was monitored using anti-HA antibodies. Glyceraldehyde 3-phosphate dehydrogenase (GAPDH) and LaminB were used as positive controls and standards for cytoplasmic and nuclear fractions, respectively. The Ptf1aK200R mutant, previously shown to be partially retained in the cytoplasm, was used as a control to assess the validity of cell fractionation protocol (Rodolosse et al., 2009). In this mutant, the lysine located 200 amino acids upstream of the start codon was replaced by an arginine. **(P)** The total extracts from DF1 cells infected with RCAS, RCAS-HA-Ptf1a and RCAS-HA-Ptf1a-Δbasic were immunoprecipitated with an anti-HA antibody. Inputs and immunoprecipitates were tested for Ptf1a or Rbpj by western blotting using anti-Ptf1a and anti-Rbpj antibodies, respectively. ONL, outer nuclear layer; INL, inner nuclear layer; IPL, inner plexiform layer; GCL, ganglion cell layer. Scale bars: 25 µm (A-J).

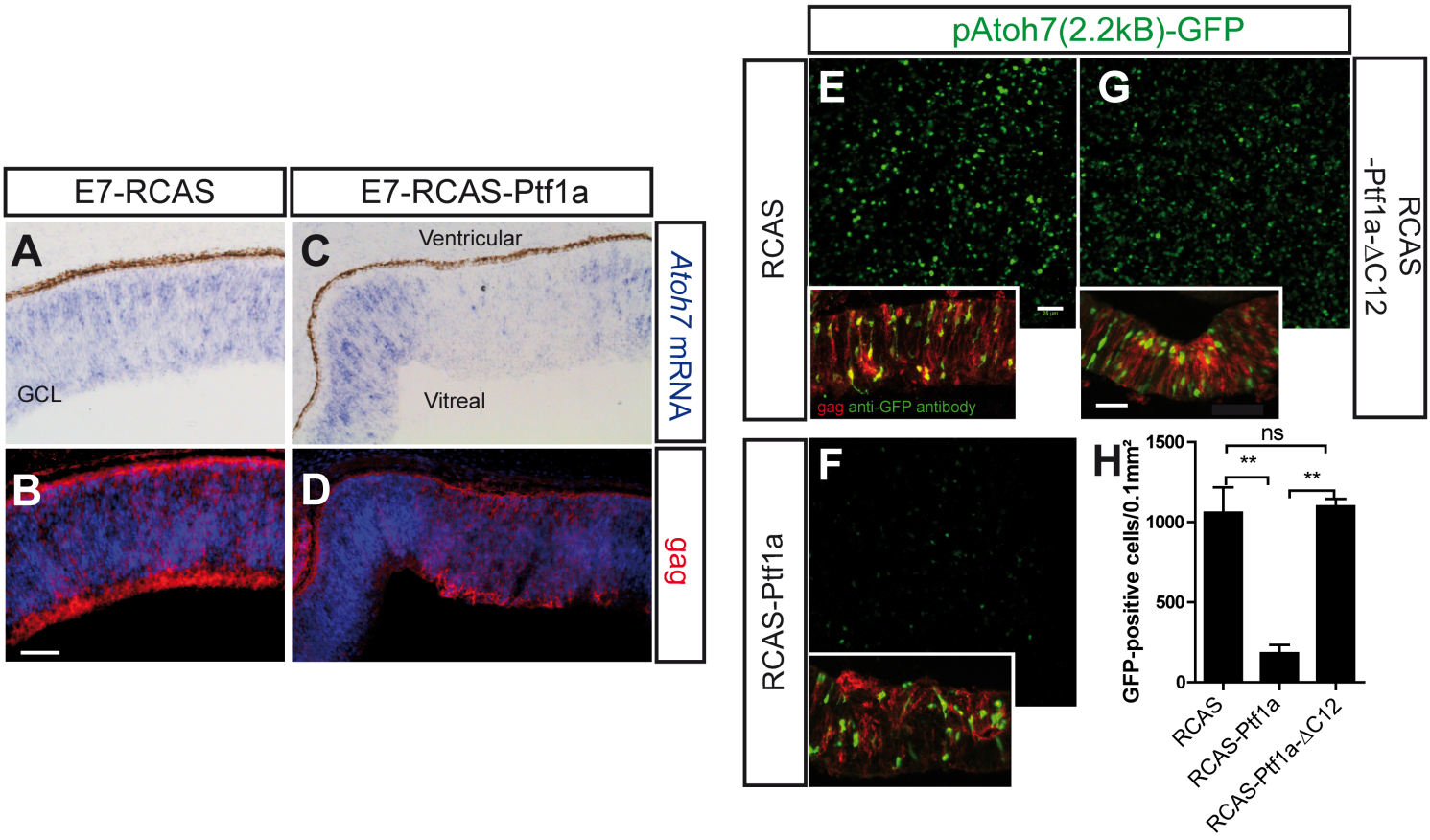

Fig. S5: Ptf1a mis/overexpression inhibits *cAtoh7* transcription.

(A-D) Sections from the RCAS-infected (A-B) and RCAS-Ptf1a-infected (C-D) retinas were hybridized at E7 with an antisense *Atoh7* riboprobe (A,C) and stained with an anti-gag (3c2) antibody (B,D) to detect the infected patches**.** The sections in B and D were counterstained with DAPI. **(E-H)** The E5 chick retinas were electroporated with pAtoh7(2.2kB)-GFP and either RCAS (E), RCAS-Ptf1a (F) or RCAS-Ptf1-ΔC12 (G) plasmids. The pAtoh7-GFP plasmid drives GFP expression in a spatiotemporal pattern that reproduces the expression of endogenous *Atoh7* gene during chick retinogenesis (Matter-Sadzinski et al., 2001; Skowronska-Krawczyk et al., 2009). After 48 h *ex vivo*, whole retinas were analyzed by confocal microscopy. Sections of electroporated retinas were immunostained using 3c2 and anti-GFP antibodies (inset) to assess the efficiency of RCAS electroporation. (H) Quantitative analysis of the number of GFP-positive cells per area (0.1 mm^2). The values represent the mean ± s.e.m of three separated retina counts and are representative of two independent experiments. GCL, ganglion cell layer. Bars : 25 µm (A-D in B), 25 µm (E-G in E, Inset: 50 µm)**.**

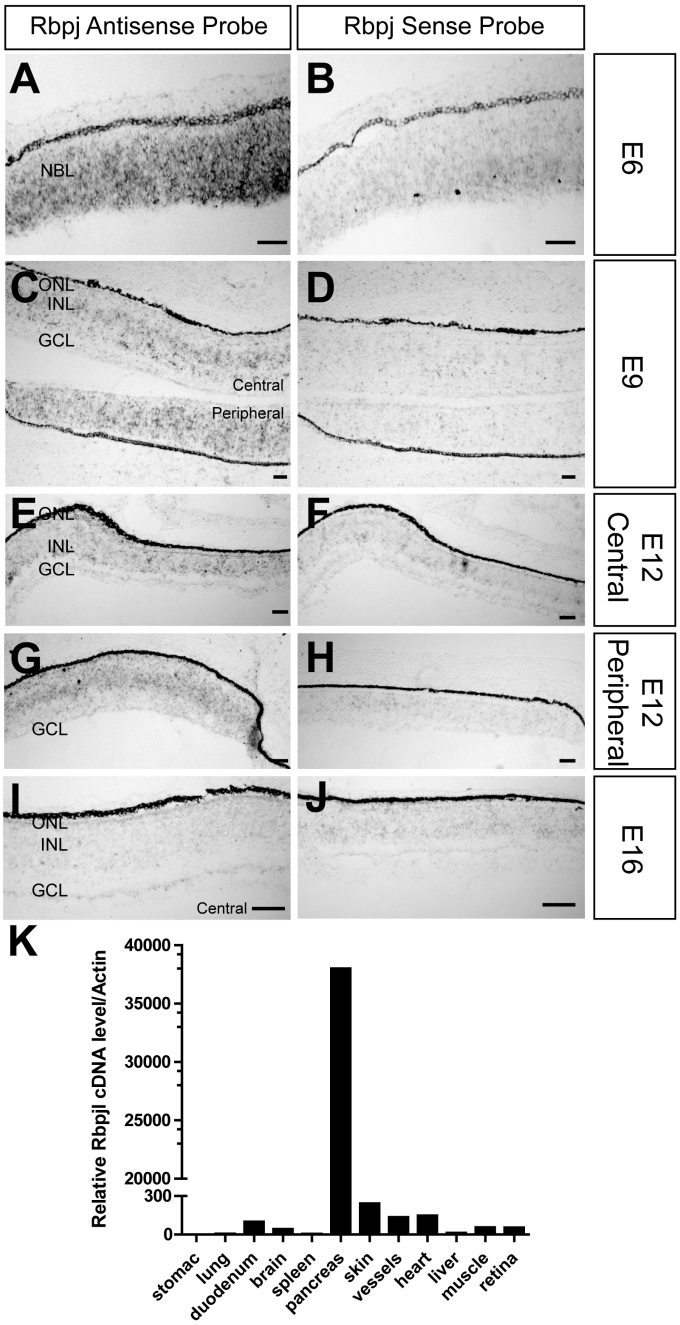

Fig. S6: Rbpj is expressed during chick retinogenesis.

(A-J) Sections from the chick retina of the indicated embryonic stages were hybridized with antisense and sense *Rbpj* riboprobes. *Rbpj* mRNA was detected within the whole retinal epithelium at E6. At E9, *Rbpj* expression was restricted to the prospective inner nuclear layer and decreased at E12 in the central retina but was higher in E12 peripheral retina. At E16, *Rbpj* expression was not detectable. **(K)** Total RNA was extracted from various organs of E19 chick embryos. *Rbpjl* mRNA levels were quantified using qPCR. *Rbpjl* was highly expressed in the chick pancreas but was not detected in the mature retina. ONL, outer nuclear layer; INL, inner nuclear layer; GCL, ganglion cell layer; NBL, neuroblastic layer. Scale bars: 20 μm (A-J).